# General Disclaimer

## One or more of the Following Statements may affect this Document

- This document has been reproduced from the best copy furnished by the organizational source. It is being released in the interest of making available as much information as possible.

- This document may contain data, which exceeds the sheet parameters. It was furnished in this condition by the organizational source and is the best copy available.

- This document may contain tone-on-tone or color graphs, charts and/or pictures, which have been reproduced in black and white.

- This document is paginated as submitted by the original source.

- Portions of this document are not fully legible due to the historical nature of some of the material. However, it is the best reproduction available from the original submission.
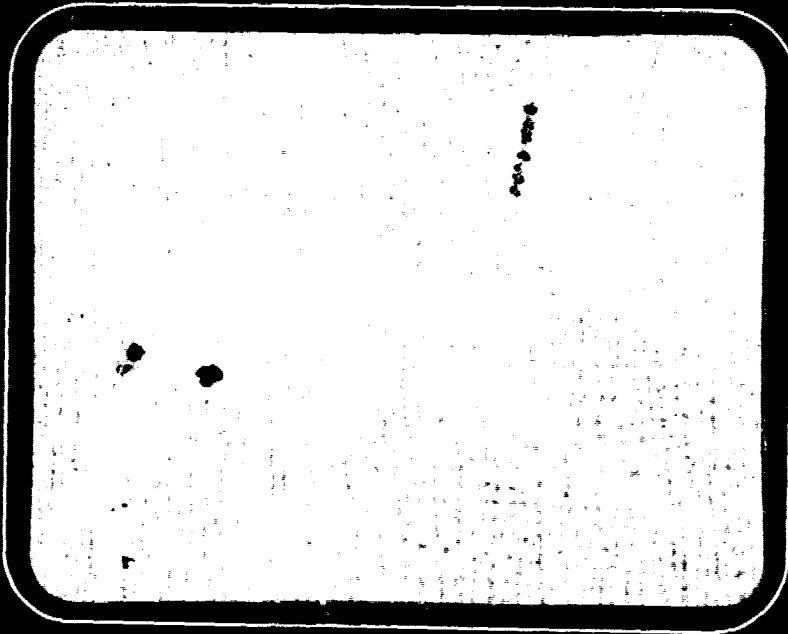
**Battelle**

Columbus Laboratories
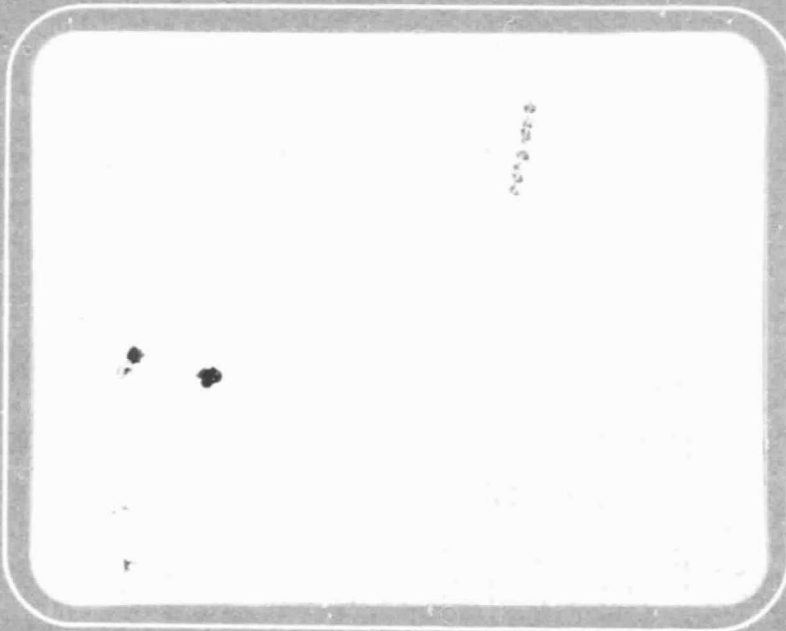
# Report

FINAL REPORT

on

HIGH PRESSURE OXYGEN TURBOPUMP
BEARING CAGE STABILITY ANALYSES
(Contract NAS8-34908 Task 113)

to

NATIONAL AERONAUTICS AND SPACE ADMINISTRATION
GEORGE C. MARSHALL SPACE FLIGHT CENTER
Marshall Space Flight Center, Alabama

March 8, 1984

by

T. L. Merriman and J. W. Kannel

# TABLE OF CONTENTS

## TABLE OF CONTENTS
### (Continued)

# HIGH PRESSURE OXYGEN TURBOPUMP
# BEARING CAGE STABILITY ANALYSES

by

T. L. Merriman and J. W. Kannel

## INTRODUCTION

Although the Space Shuttle has repeatedly had successful launches, the life of the engine bearings remains below the overall program objectives. Because the shuttle is a reusable spacecraft, the target life of the turbopump bearings of the Space Shuttle main engine (SSME) has been raised from a few hundred seconds for single-use rockets to 7.5 hours for the shuttle application. In addition, the bearings are required to operate at very high speeds and with poor lubrication conditions. The lubrication must be derived from cryogenic hydrogen or oxygen and/or by transfer from the cage material (PTFE).

A the high pressure oxygen turbopump (HPOTP) bearing on the turbine end (No. 007955) failed recently in a test engine operating at conditions which simulate the SSME requirements. The cause of this failure is uncertain, but excessive ball wear and fracture of the cage was observed. One of the major questions to be resolved is whether the bearing cage failed under normal loading or whether dynamic cage instability caused the cage failure from associated excessive loads.

Battelle has been assisting NASA in development of the SSME bearings through a Task Order Agreement. The objective of this Task was to evaluate whether the dynamic stability of the SSME HPOTP turbine-end bearing cage is an important factor in the failures. This was accomplished by analysis with the Battelle "BASDAP" bearing computer stability model. The intent was to vary particular individual parameters over specified ranges to determine the dynamic sensitivity of the cage to each parameter.

## SUMMARY AND CONCLUSIONS

Combinations of operating conditions and cage dimensions were identified that can cause the cage of the HPOTP turbine-end bearings to be unstable. Furthermore, the high accelerations associated with the instabilities can be expected to cause forces sufficient to fail the cage (depending upon the actual strength of the cage under operating conditions). The forces on the cage developed under normal (stable) operating conditions were found to be tolerable. Therefore, maintaining stable operation of the cage appears to be important in successful operation of the HPOTP bearings.

Cage stability was found to be particularly sensitive to the cage-race clearance, cage balance, and the lubricant film thickness between the balls and races (as it affects the ball-race traction). Cage-race diametral clearances larger than 0.25 mm (0.01 in.) promote cage instabilities. In contrast, cage stability was found to be insensitive to ball-pocket clearance. Since small cage unbalances were predicted to cause instabilities, the cages should be carefully balanced to minimize instability problems. Depletion of lubricant film thicknesses between the balls and races cause cage instability problems by increasing the ball-race traction, which underlines the importance of maintaining adequate lubrication for successful long-term bearing life.

As a result of the study, several sensitive parameters affecting bearing dynamics were clearly identified. Therefore, modifications to the bearings to minimize the likelihood of cage instability should enhance cage stability and associated bearing reliability.

## RECOMMENDATIONS

Based on the analyses, the following specific recommendations are made to minimize cage instability and its associated effects on bearing degredation.

1. Maintain the diametral cage-race clearance
   at no more than 0.25 mm (0.010 in.). Current
   specifications on the drawing of bearing 007955
   for cage-race clearance are 0.38 mm (0.015 in.)
   to 0.74 mm (0.029 in.). This tolerance should
   be changed to reflect the 0.25 mm (0.010 in.)
   maximum allowable recommendation.

2. The clearance between the balls and pockets
   in the cage should be no less than 0.54 mm
   (0.025 in.). The ball-pocket clearance does
   not affect cage stability, but adequate clearance
   is needed to avoid cage stresses from ball-speed
   variations caused by combinations of axial
   and radial loads. It is recommended that
   the current drawing specification of 0.64 mm
   (0.25 in.) to 0.89 mm (0.035 in.) for ball-pocket
   clearance in the circumferential direction
   be modified to be 2.3 mm (0.090 in.) to 2.5 mm
   (0.100 in.) to reflect this requirement.

3. Dynamically balance the cages to minimize
   the effect of cage unbalance on stability.

4. Continue efforts to understand and promote
   adequate lubrication of the ball-race interface.
   This analysis has shown the importance of
   lubrication to cage stability, and previous
   Tasks have underscored the importance of
   lubrication to ball and race longevity.
   Long-term life of the HPOTP bearings depends
   critically on developing and maintaining
   lubricant films to separate the balls and
   races.

5. Perform a more detailed analysis of the cage
   stresses developed in operation. While the
   BASDAP analyses provide data on the ball-cage

forces, the actual stresses developed result
from a combination of these forces with the
cage geometry and constraints by the outer
(guiding) race. The current study permitted
only an approximate consideration of these
stresses.

6. Schedule a review meeting to be attended
   by NASA, Rocketdyne, and Battelle personnel
   to review the implications of the findings
   in this Task and determine what practical
   steps can be taken to minimize potential
   cage instability problems.


## CAGE-STABILITY ANALYSES BACKGROUND


### Ball-Race Interactions

An angular contact bearing contains three types of elements:
   (1)  Balls,
   (2)  Races (inner and outer), and
   (3)  Ball cage (retainer).

External loading in the bearing develops loads at the ball-race inter-
faces. These forces, along with race geometry, speed, and centrifugal
effects, produce the ball-race contact angles, ball-race contact pressures,
lubricant film thickness (between balls and race), and to some extent,
the spin and roll motions of the ball. The analysis of these ball-race
interactions was the basis for the classical A. B. Jones' theory[1]*.

The Jones' approach involves first computing the spring rates
for the ball-race contact regions. Next, values for the radial and axial
deflections of the bearing are assumed. Using these assumed deflections
in conjunction with the spring rates, radial and axial loads are computed
and compared with the design bearing loads. The radial and axial deflec-
tions are adjusted (by a computer nesting procedure) to achieve the

---

*References are listed on page 32.

correct loads for static conditions. Centrifugal force effects are determined by adjusting the inner and outer race contact angles to achieve loading equilibrium.

## Cage Dynamics

Under design (static) conditions of most bearings, the cage can be considered to have six degrees of freedom. The motion of the cage is achieved as a result of the balls driving the cage or the cage driving the balls. The stability conditions of the cage are a result of the interactions during ball-cage impacts. As a result of this impact, the kinetic energy of the cage is altered. For example, any slip of the ball on the race at impact will reduce the energy of the cage. Also, the friction coupling of the rolling ball to the cage during impact alters the cage energy. Under some conditions, the energy of the cage will continue to increase until an instability occurs. Under other conditions, the cage will be quite stable. The purpose of the BASDAP model is to sort out these stable or unstable conditions.

The BASDAP calculations are conducted in two steps:

Step 1.  The quasi-dynamic stresses of the type discussed under "Ball-Race Interactions of the Bearing" are computed.

Step 2.  The cage dynamic motions are computed using the ball-race forces and traction constants as inputs. This model is described in the paper presented in Appendix B.

Cage motion is computed in terms of three velocity components $\dot{\alpha}$, $\dot{\beta}$, and $\dot{\rho}$. $\alpha$, $\beta$, and $\rho$ are described in Figure B-1. $\dot{\alpha}$ represents the angular rotation of the cage. Under perfect conditions, $\dot{\alpha}$ would be the same as the ball group velocity although normally some oscillations relative to the group velocity occurs. In the plots (to be discussed), $\dot{\alpha}$ will be shown relative to the ball group. $\dot{\beta}$ represents the whirl velocity of the cage center-of-mass relative to the geometric center of the bearing.

$\overset{\bullet}{\rho}$ represents the cage radial velocity. Cage stability can be accessed by analyzing plots of $\alpha$ (cage angle) as a function of time. If the frequency of oscillation of $\alpha$ decreases with time, cage stability is implied. Conversely, if the frequency of oscillation increases, the cage is unstable.

## CAGE-STABILITY ANALYSIS

In the analyses, only one parameter was varied at a time. The nominal bearing parameters used, while any given parameter was varied, are listed in Table 1. The ranges over which the parameters were varied are listed in Table 2. Because of the very large number of possible combinations, no attempt was made to perform a complete analysis of the interactions of the variables.

In presenting the results, bar graphs were made to summarize the effect of the particular variable of interest. The detailed computer-generated plots of cage motion and cage velocity, on which the bar graphs were based, are presented in Appendix A. In interpreting the bar graphs, the following definitions should be used.

Completely unstable - high frequency oscillation.

Marginally unstable - occasional oscillation build up.

Marginally stable - oscillations do not completely decay, but the cage does not go into high frequency oscillation.

Stable - frequency and amplitude of oscillation decrease with time.

### Cage-to-Outer-Race Clearance

The effect of cage-to-outer-race diametral clearance on cage stability is presented in Figure 1, and the detailed computer graphs are presented in Figure A-1. Stable operation is attained at clearances of 0.25 mm (0.010 in.), marginal stability is predicted at 0.51 mm (0.020 in.), and unstable cage operation is predicted for clearances of 0.76 mm (0.030 in.) and greater. Therefore, the cage-race clearance should not exceed 0.25 mm (0.010 in.) for stable cage operation with the values of the parameters given in Figure 1.

TABLE 1.   NOMINAL BEARING PARAMETERS FOR NASA BEARING 007955
            (HPOTP, TURBINE END)

| Parameter | Units | Nominal Value |
|---|---|---|
| Number of Balls | -- | 13 |
| Ball Radius | mm (inch) | 6.35 (0.250) |
| Pitch Radius | mm (inch) | 40.51 (1.595) |
| Design Contact Angle | rad/degrees | 0.36/20.5 |
| Outer Race Curvature | -- | 0.53 |
| Inner Race Curvature | -- | 0.53 |
| Ball-Race Friction Coefficient | -- | 0.13 |
| Ball-Cage Friction Coefficient | -- | 0.30 |
| Axial Load | N (lb) | 4448 (1000) |
| Radial Load | N (lb) | 2669 (600) |
| Inner Race Speed | rpm | 31,000 |
| Cage Mass | gm (lb-sec$^2$/in.) | 29.78 (1.730 x $10^{-4}$) |

TABLE 2.  BEARING PARAMETER RANGES FOR NASA BEARING
007955 (HPOTP, TURBINE END)

| Parameter | Range |
|---|---|
| Ball-Pocket Clearance | 0.635 mm to 2.54 mm<br>(0.025 in. to 0.100 in.) |
| Cage to Outer Race Clearance | 0.254 mm to 1.52 mm<br>(0.010 in. to 0.060 in.) |
| Ball to Ball-Pocket Friction | 0.04 to 0.30 |
| Cage to Outer Race Friction | 0.04 to 0.30 |
| Ball to Race Friction | 0.08 to 0.22 |
| Shaft Speed | 25,000 rpm to 31,000 rpm |
| Bearing Loads (per bearing)<br>1000# Axial | 890 N to 4448 N<br>(200 lb to 1000 lb) |
| Bearing Film Thickness | $2.54 \times 10^{-4}$ to $24.9 \times 10^{-4}$ mm<br>($10 \times 10^{-6}$ to $98 \times 10^{-6}$ in.) |
| Cage Weight | 29.00 to 29.78 gram |
| Cage Unbalance | 0 to 0.5 gram |
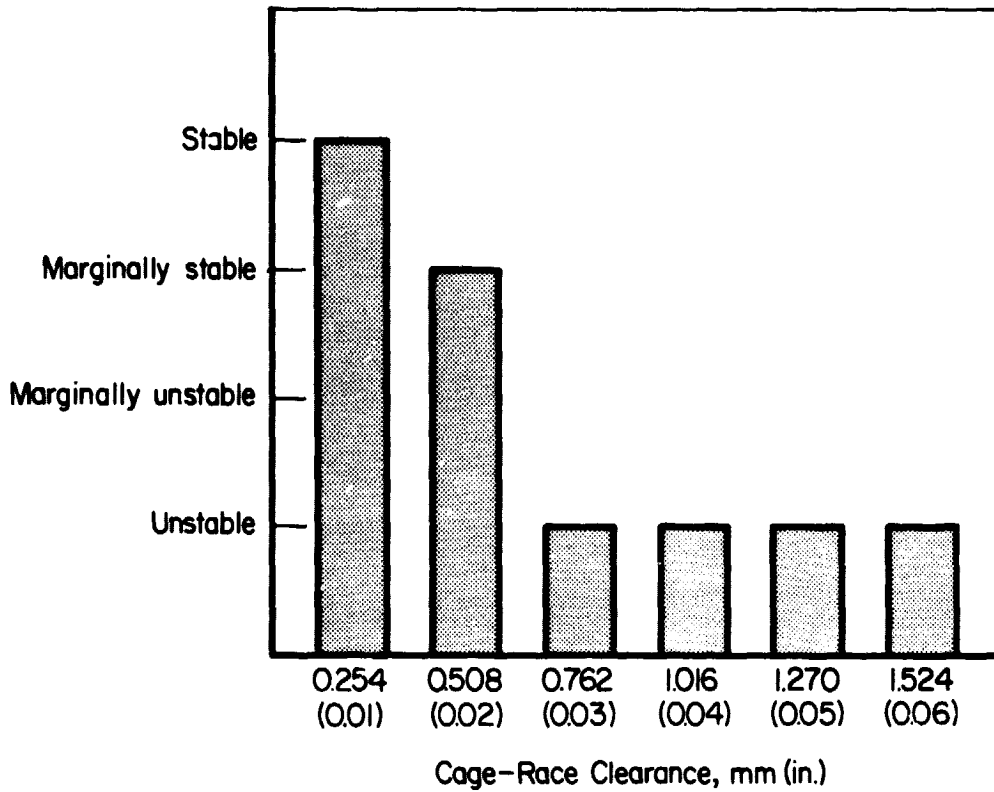
FIGURE 1.   CAGE STABILITY AS A FUNCTION
OF CAGE-RACE CLEARANCE

Axial Load = 4448 N (1000 lb)        Radial Load = 2669 (600 lb)
Cage-Rac_ Friction = 0.13            Ball-Cage Friction = 0.30
Cage-Race Clearance = Variable       Ball-Cage Clearance = 0.635 mm
Speed = 31,000 rpm                        (0.025 in.)

## Ball-Pocket Clearance

Figure 2 presents the effects of ball-cage diametral clearance
on cage stability. In general, increasing ball cage clearance does not
cause serious deteriorations of cage stability for a cage-race clearance
of 0.259 mm (0.010 in.). The computer graph in Figure A-2b does illustrate
that some cage wobbling may be occurring, which is a reflection of the
cage impacting the race guiding surface. Figure A-2c shows that a very
low frequency impact occurs, but it is unlikely that these motions represent
a stability problem.

## Cage-to-Outer-Race Friction

Figure 3 shows the effect of cage-race friction coefficient
ranging from a very low value of 0.04 to a high of 0.30 (the maximum
value experimentally reported for Armalon sliding against 440 C stainless
steel in liquid nitrogen). An increasing coefficient of friction at
the cage-race interface should tend to stabilize the bearing as cage
and ball group energy is dissipated through the race land in the form
of heat, and this tendency was observed. The corresponding computer
plots are presented in Figure A-3.

## Ball to Ball-Pocket Friction

Figure 4 shows the effect of the ball-cage friction coefficient
over the same range of 0.04 to 0.30. Increasing the coefficient of friction
at this interface would normally be expected to decrease bearing stability
as more energy is transferred to the cage. The plots, however, do not
show a strong effect of varying the ball-cage friction alone for this
bearing geometry.

Experimental data provided by the Marshall Space Flight Center
Materials Laboratory shows that as the cage wears the coefficients of
friction at the race and ball interfaces change preferentially with regard
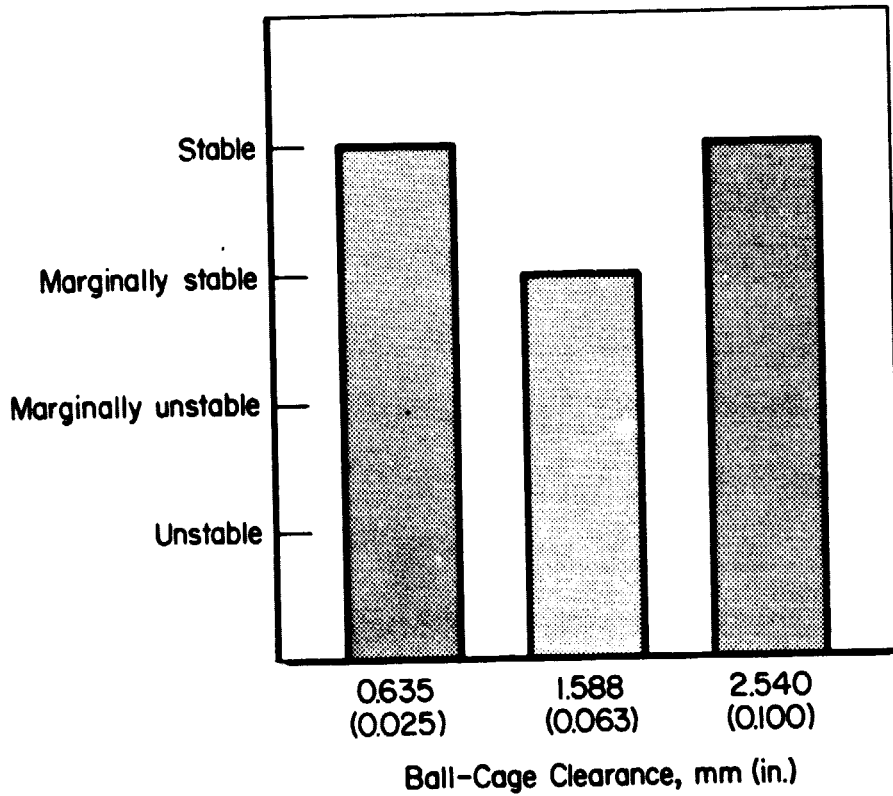to cage fiber orientation. The ball-cage interface wears perpendicular

FIGURE 2. CAGE STABILITY AS A FUNCTION
OF BALL-CAGE CLEARANCE

Axial Load = 4448 N (1000 lb)          Radial Load = 2669 (600 lb)
Cage-Race Friction = 0.13              Ball-Cage Friction = 0.30
Cage-Race Clearance = 0.254 mm         Ball-Cage Clearance = Variable
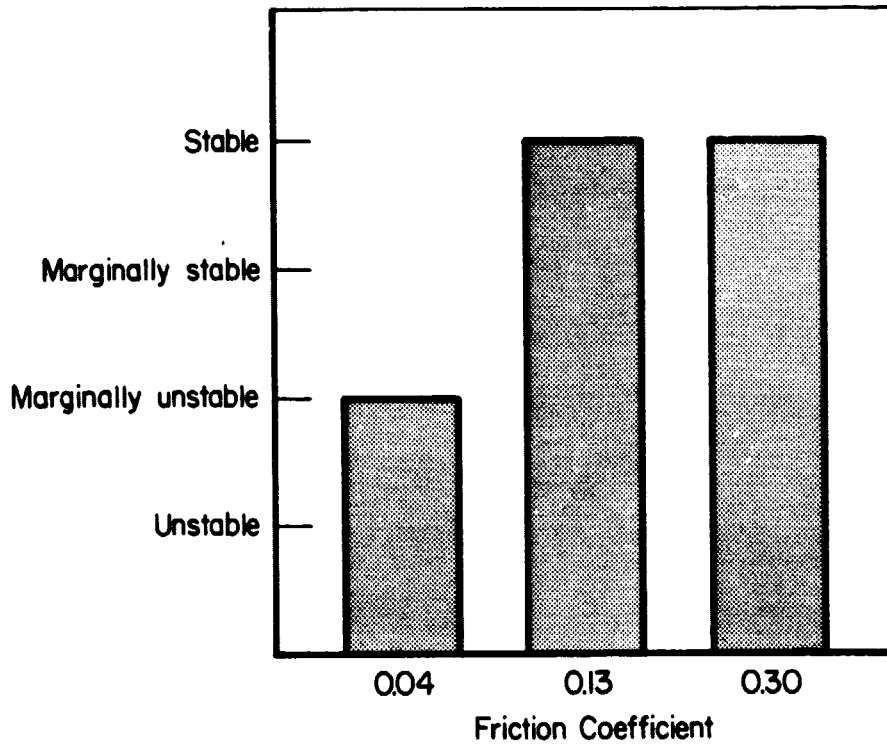    (0.010 in.)                        Speed = 31,000 rpm

FIGURE 3.   CAGE STABILITY AS A FUNCION
OF CAGE-RACE FRICTION

Axial Load = 4448 N (1000 lb)
Cage-Race Friction = Variable
Cage-Race Clearance = 0.254 mm
    (0.010 in.)
Speed = 31,000 rpm

Radial Load = 2669 (600 lb)
Ball-Cage Friction = 0.30
Ball-Cage Clearance = 0.635 mm
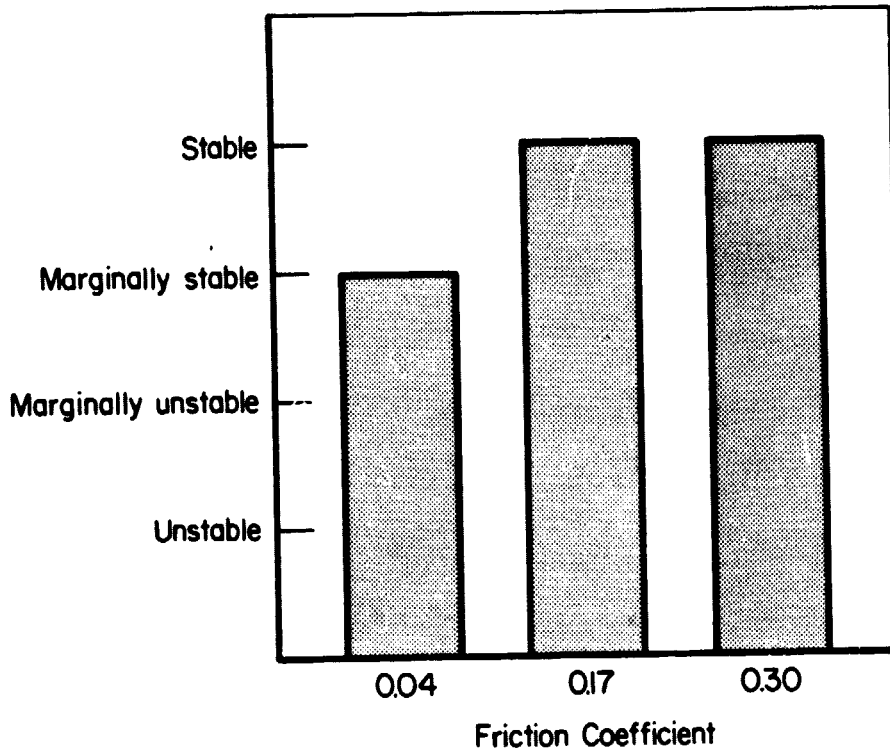    (0.025 in.)

FIGURE 4. CAGE STABILITY AS A FUNCTION
OF BALL-CAGE FRICTION

Axial Load = 4448 N (1000 lb)
Cage-Race Friction = 0.13
Cage-Race Clearance = 0.254 mm
    (0.010 in.)
Speed = 31,000 rpm

Radial Load = 2669 (600 lb)
Ball-Cage Friction = Variable
Ball-Cage Clearance = 0.635
    (0.025 in.)

to the lay of the cage fiber and the coefficient of friction tends to increase to 0.30. The cage guiding surface wears parallel to the lay of the cage fiber and the coefficient of friction tends to decrease slightly to 0.13 at the higher loads. This combination of friction coefficients was analyzed and is represented in Figure A-3b, which is a stable plot. The experimental data from which these friction coefficients were taken is presented in Table 3. The worst combination of friction coefficients would be : high ball-cage (0.30) and a low cage-race value (0.04). Running this combination produced a marginally stable cage, presented in Figure A-3a. From these results, the coefficients of friction at the ball-cage and race-cage interfaces do not have a strong influence on cage stability.

## Cage Unbalance

Stability appeared to be sensitive to cage unbalance, as shown in Figure 5 and in the computer plots in Figure A-5. Unstable operation was predicted with unbalances of only 0.019 grams at the cage radius of 41 mm (1.63 in.), or, 0.078 g-cm. At 13,400 rpm, this unbalance corresponds to a force of $1.55 \times 10^5$ dynes (0.35 pounds), or 160 $g_f$, which is approximately 5 times greater than the cage "weight" of 30 g (0.066 pounds). These forces possibly contribute to initiating and maintaining instability in the absence of other dominating effects.

The results suggest that the cages should be balanced if this is not currently being done. Balancing equipment is available for detecting at least 0.008 g-cm, or one tenth the unbalance used in the analyses The studies did not include determining maximum allowable unbalances for stability. However, the cage should be balanced as well as possible.

## Radial Load

The effect of radial load was determined at load 890, 2669, and 4448 N (200, 600, and 1000 pounds), shown in Figure 6 and in the computer plots in Figure A-6. At 890 N (200 pounds) the amplitude of oscillation appears to grow steadily, perhaps to the point of instability.

TABLE 3. EXPERIMENTAL FRICTION COEFFICIENT FOR BEARING CAGE
MATERIAL ON BEARING RACE MATERIAL AT LIQUID NITRO-
GEN TEMPERATURE

| TEST MATERIAL | | | | | |
|---|---|---|---|---|---|
| Pellet | | Plate | | | |
| Armalon Fiber Orientation | | Surface Finish = $50.8 \times 10^{-6}$ mm $(2 \times 10^{-6}$ in.) | | | |
| (1) Plies Parallel to Plate | | (a) 440C Stainless Steel | | | |
| (2) Plies Perpendicular to Plate | | | | | |
| Pellet-Plate Combination | Load $N/m^2 \times 10^6$ (psi) | Static Friction Old | New | Dynamic Friction Old | New |
| 1-a | 1.38 (200) | 0.139 | 0.324 | 0.109 | 0.189 |
| 1-a | 3.45 (500) | 0.131 | 0.242 | 0.102 | 0.145 |
| 1-a | 6.89 (1000) | 0.140 | 0.177 | 0.102 | 0.125 |
| 2-a | 1.38 (200) | 0.135 | 0.254 | 0.109 | 0.169 |
| 2-a | 3.45 (500) | 0.214 | 0.389 | 0.160 | 0.311 |
| 2-a | 6.89 (1000) | 0.243 | 0.344 | 0.167 | 0.300 |
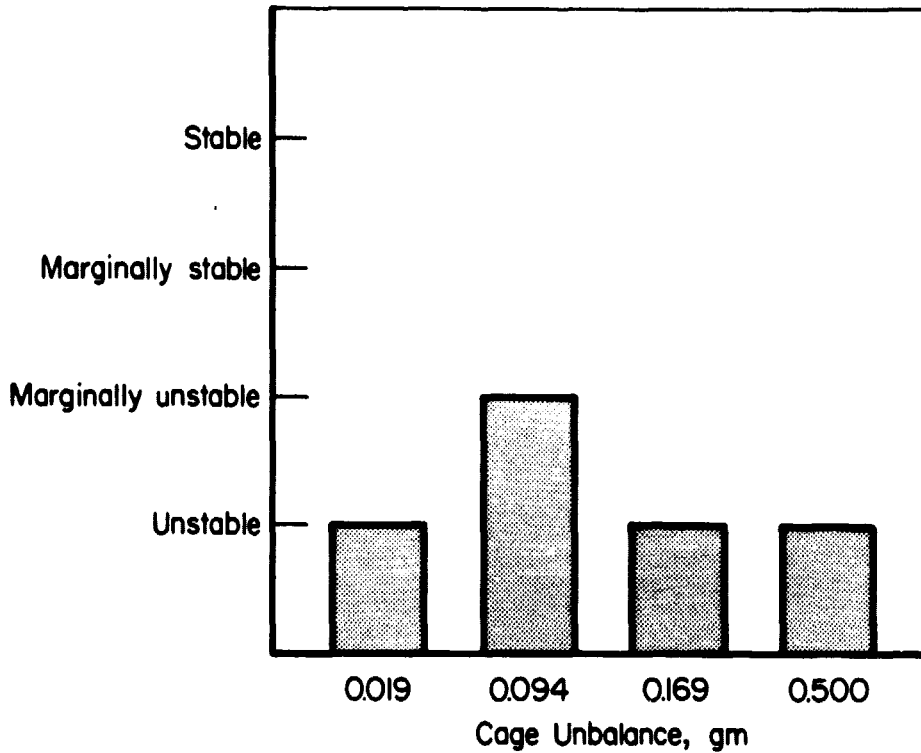
FIGURE 5.   CAGE STABILITY AS A FUNCTION
OF CAGE UNBALANCE

Axial Load = 4448 N (1000 lb)
Cage-Race Friction = 0.13
Cage-Race Clearance = 0.254 mm
    (0.010 in.)
Speed = 31,000 rpm

Radial Load = 2669 (600 lb)
Ball-Cage Friction = 0.30
Ball-Cage Clearance = 0.635 mm
    (0.025 in.)
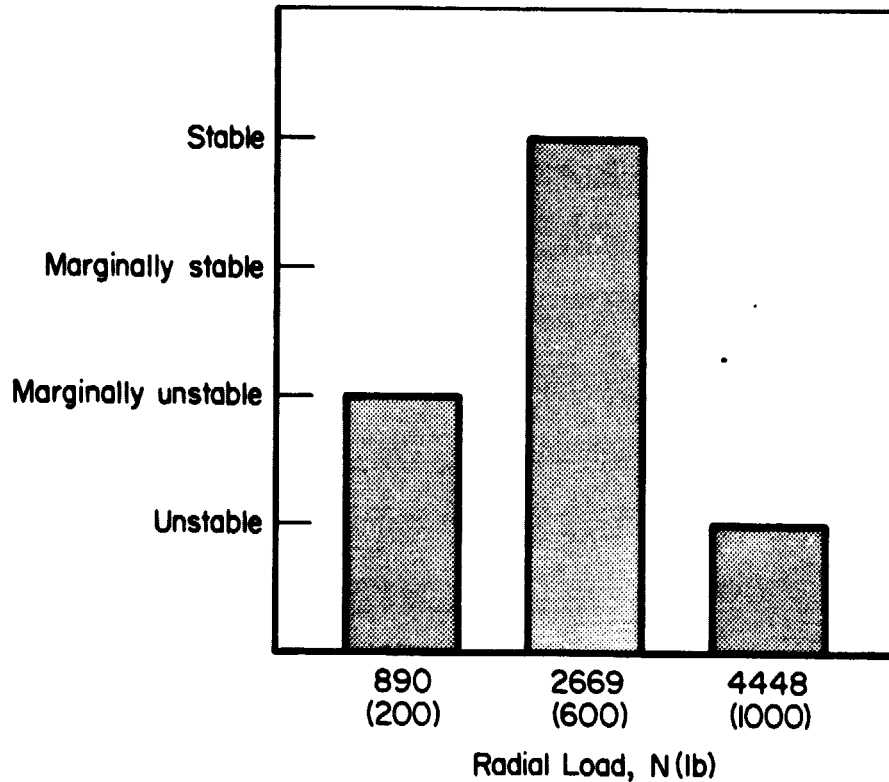
FIGURE 6.   CAGE STABILITY AS A FUNCTION
OF RADIAL LOAD

Axial Load = 4448 N (1000 lb)               Radial Load = Variable
Cage-Race Friction = 0.13                    Ball-Cage Friction = 0.30
Cage-Race Clearance = 0.254 mm               Ball-Cage Clearance = 0.635 mm
   (0.010 in.)                                  (0.025 in.)
Speed = 31,000 rpm

With the radial load raised to 2669 N (600 pounds), the cage was stable. However, at the higher radial load of 4448 N (1000 pounds), the cage again became unstable. The reason for this intermediate range of stability was not determined.

## Cage Mass

Small changes in cage mass had little effect on the cage stability from the nominal case, Figure 7, with the computer plots presented in Figure A-7.

## Shaft Speed

The effect of varying the shaft speed on cage stability was studied from 25,000 to 31,000 rpm, Figure 8, with the computer plots in Figure A-8. These plots show that the bearing is only marginally stable since small changes in speed cause a change in predicted stability, which is qualitatively similar to experience. Quantitatively, the results are somewhat counter to experience that shows bearing problems at higher speeds. However, it should be noted that bearing dynamics calculations are based on single variable evaluations. In reality, many variables change simultaneously. The conclusion is that the bearing speed is near the thresho'd of instability.

## Transferred Lubricant Film Thickness

The film thicknesses used were assumed to be PTFE solid films transferred presumably from the cage. The presence of ball-race lubricant films influences stability by affecting the ball-race coefficient of friction and therefore the ability for balls to skid on the race. The relationship between film thickness and coefficient of friction (traction) was obtained from other Battelle experiments on this topic. As would be expected, the thicker films promote stability, Figure 9, with the computer graphs in Figure A-9. Films $2.5 \times 10^{-3}$ mm ($98 \times 10^{-6}$ in.)
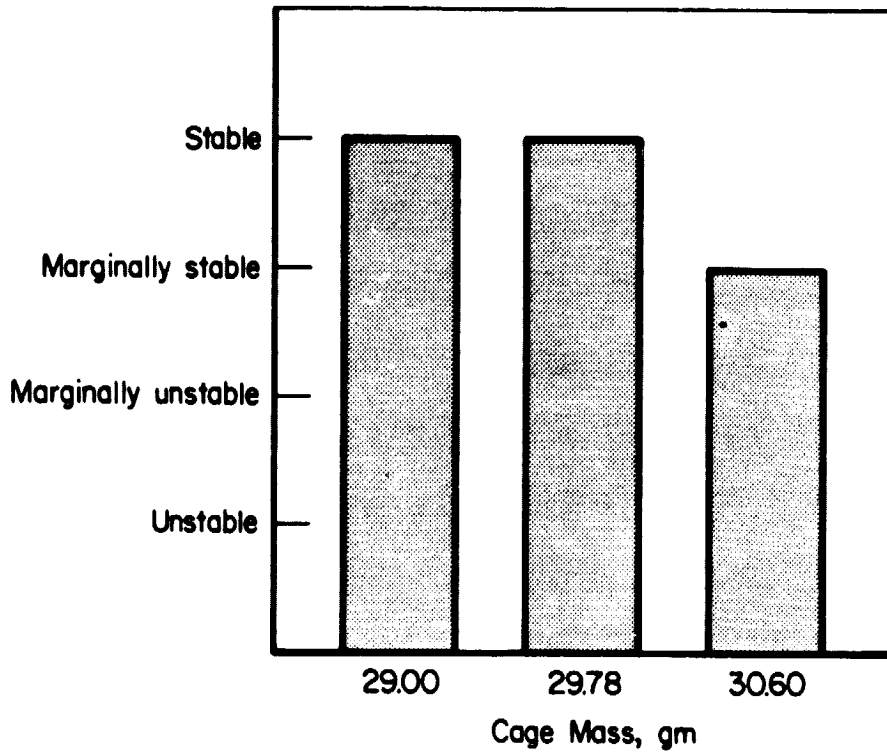
FIGURE 7.  CAGE STABILITY AS A FUNCTION
OF CAGE MASS

Axial Load = 4448 N (1000 lb)
Cage-Race Friction = 0.13
Cage-Race Clearance = 0.254 mm
    (0.010 in.)
Speed = 31,000 rpm

Radial Lcad = 2669 N (600 lb)
Ball-Cage Friction = 0.30
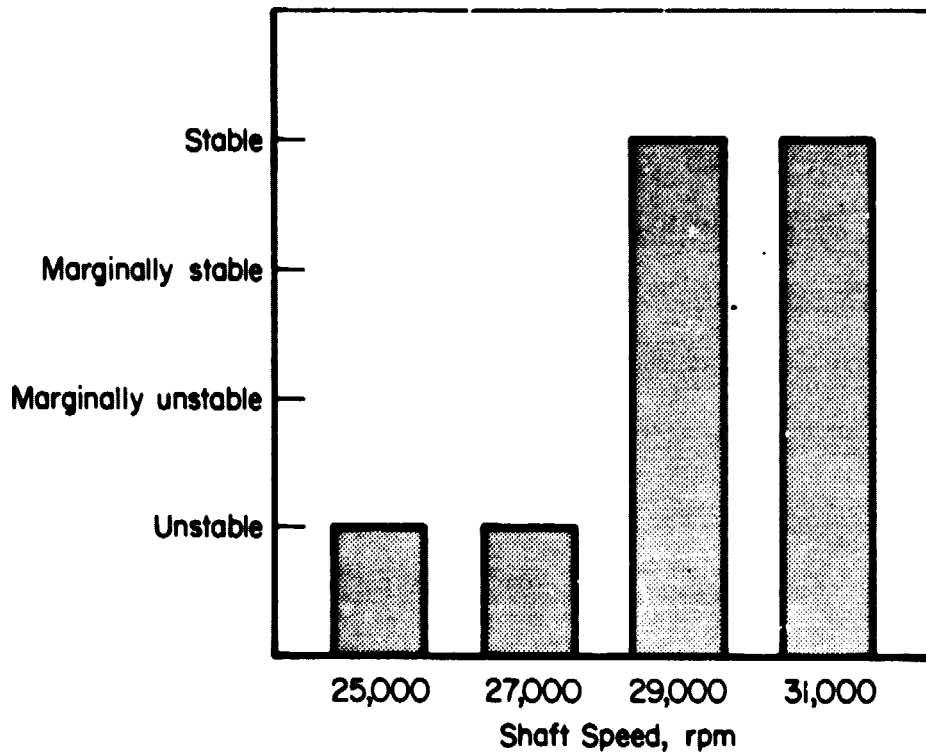Ball-Cage Clearance = 0.635 mm
    (0.025 in.)

FIGURE 8.   CAGE STABILITY AS A FUNCTION
OF SHAFT SPEED

Axial Load = 4448 N (1000 lb)
Cage-Race Friction = 0.13
Cage-Race Clearance = 0.254 mm
     (0.010 in.)
Speed = Variable

Radial Load = 2669 N (600 lb)
Ball-Cage Friction = 0.30
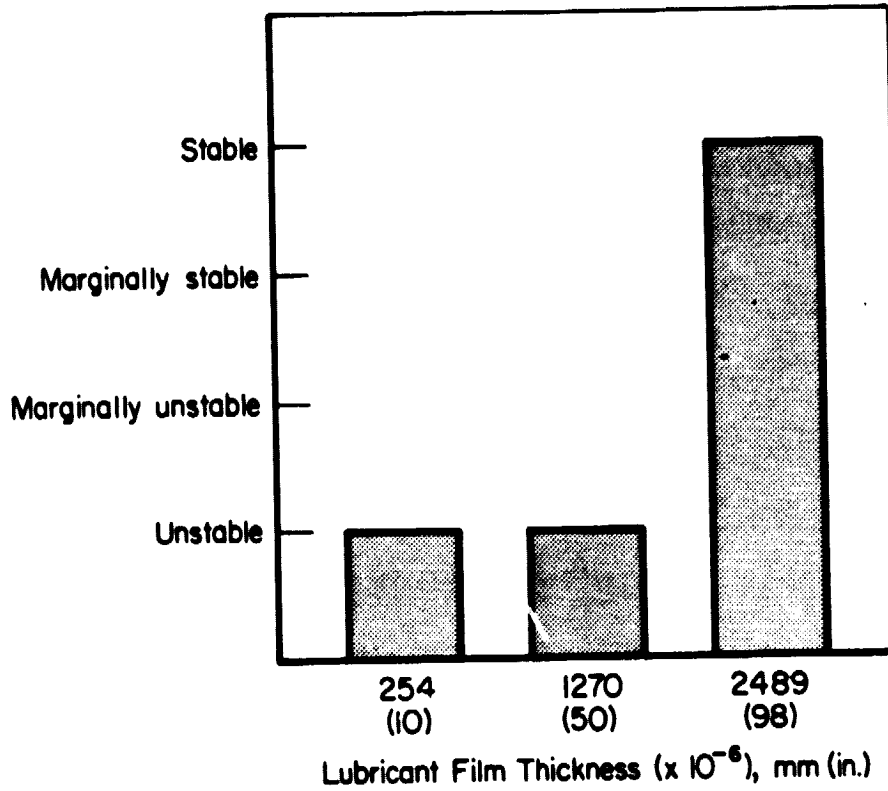Ball-Cage Clearance = 0.635 mm
     (0.025 in.)

FIGURE 9.   CAGE STABILITY AS A FUNCTION OF LUBRICANT
TRANSFER FILM EFFECTIVE THICKNESS

Axial Load = 4448 N (1000 lb)
Cage-Race Friction = 0.13
Cage-Race Clearance = 0.254 mm
     (0.010 in.)
Speed = 31,000 rpm

Radial Load = 2669 N (600 lb)
Ball-Cage Friction = 0.30
Ball-Cage Clearance = 0.635 mm
     (0.025 in.)

thick prcduced a stable case, while thickness reductions of 50 percent and greater produced instability. This analysis did not consider possible contributions of elastohydrodynamic films generated by the liquid oxygen.

## CAGE LOADING ANALYSIS

### Cage Strength

A consideration of cage loading that may cause failures requires a knowledge of the cage strengths to determine whether sufficient forces are being developed at the ball-cage interfaces to exceed the ultimate cage strength. Tensile stress data were provided on the cage material by NASA for two fiber orientations over a range of temperatures, but the relationship of the orientation to the actual cage was unclear. As a simple check on whether the data translated into appropriate strengths at room temperature, several sections were pulled to failure in the tensile set-up shown in Figure 10. Since the sides of the ball-pockets were formed by drilling holes into the cage, the sides of an individual pocket are parallel and perpendicular to the minimum cross sectional area of the cage. Pulling in the manner shown in Figure 10, therefore, introduces bending stresses into the cage section that may not normally be seen in service. Also, the loops were smaller than a ball in diameter, which produced a stress concentration at the point of contact. The results from eight specimens at room temperature indicated a strength of $600 \pm 22$ N ($135 \pm 5$ pounds). This results in a calculated stress of 40 N/mm$^2$ (5700 psi), which includes the expected bending stresses from the curved geometry. One additional experiment was conducted with 12.7 mm (0.5 in.) rods in adjacent ball pockets, which therefore included the thin sections of two ball pockets in the tensile field. A higher strength of 800 N (180 pounds) was recorded in this test in spite of the higher bending stresses produced. The calculated maximum stress was approximately 160 N/mm$^2$ (23,000 psi). This value falls between the NASA-supplied ultimate-tensile-strength data for "with fabric" and "through fabric" of 83 N/mm$^2$
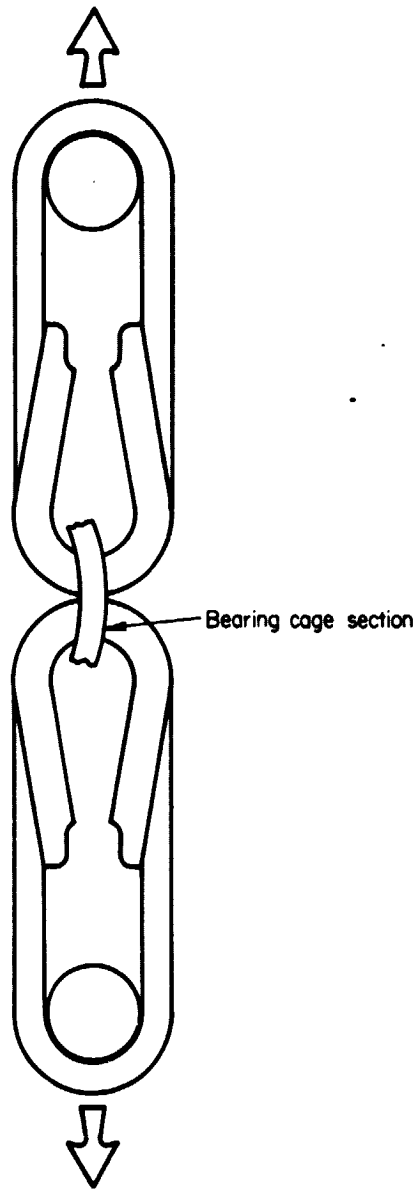
FIGURE 10.   ULTIMATE STRENGTH TEST OF CAGE SECTION

(12,000 psi) and 210 N/mm$^2$ (30,000 psi), respectively. Therefore, for the purposes of this stuay, the lower strength levels were assumed to apply. At -196 C (-320 F), the tension and compression strength data were:

Utlimate tensile stress = 270 N/mm$^2$ (39,000 psi)
Ultimate force in pure tension = 6900 N (1600 pounds)
Ultimate compressive stress = 230 N/mm$^2$ (33,000 psi)
Ultimate force in pure compression = 5900 N (1300 pounds)

## Cage Stresses Under Normal Operating Conditions

The cage in a ball bearing maintains the ball spacing, which would otherwise become non-uniform in service from a variety of operating conditions and geometric imperfections. Examples include ball unloading, ball diameter variations, and rapid speed changes. Therefore, the cage must be capable of applying sufficient force to a ball to cause it to skid on the races and thereby maintain its nominal location. The force required is a function of the ball-race coefficient of friction and the applied ball load. Varying the ball loading by varying the axial load will therefore result in different maximum forces that must be applied by the cage to the balls.

The effect of varying the axial load and the ball-race coefficient of friction on the maximum cage forces is presented in Figure 11 for a bearing operating under normal conditions (stable cage). The maximum cage forces increase, as expected, with coefficient of friction and axial load. With an axial load of 4400 N (1000 pounds) and a coefficient of friction of 0.22, the maximum ball-cage force was calculated to be 300 N (67 pounds). This force is well below the ultimate forces for cage failure of 6900 N (1600 pounds) in tension and 5900 N (1300 pounds) in compression. The cage could also withstand much higher axial forces being applied to the bearing. An order-of-magnitude increase in axial force would be required before the cage would become subject to failure.
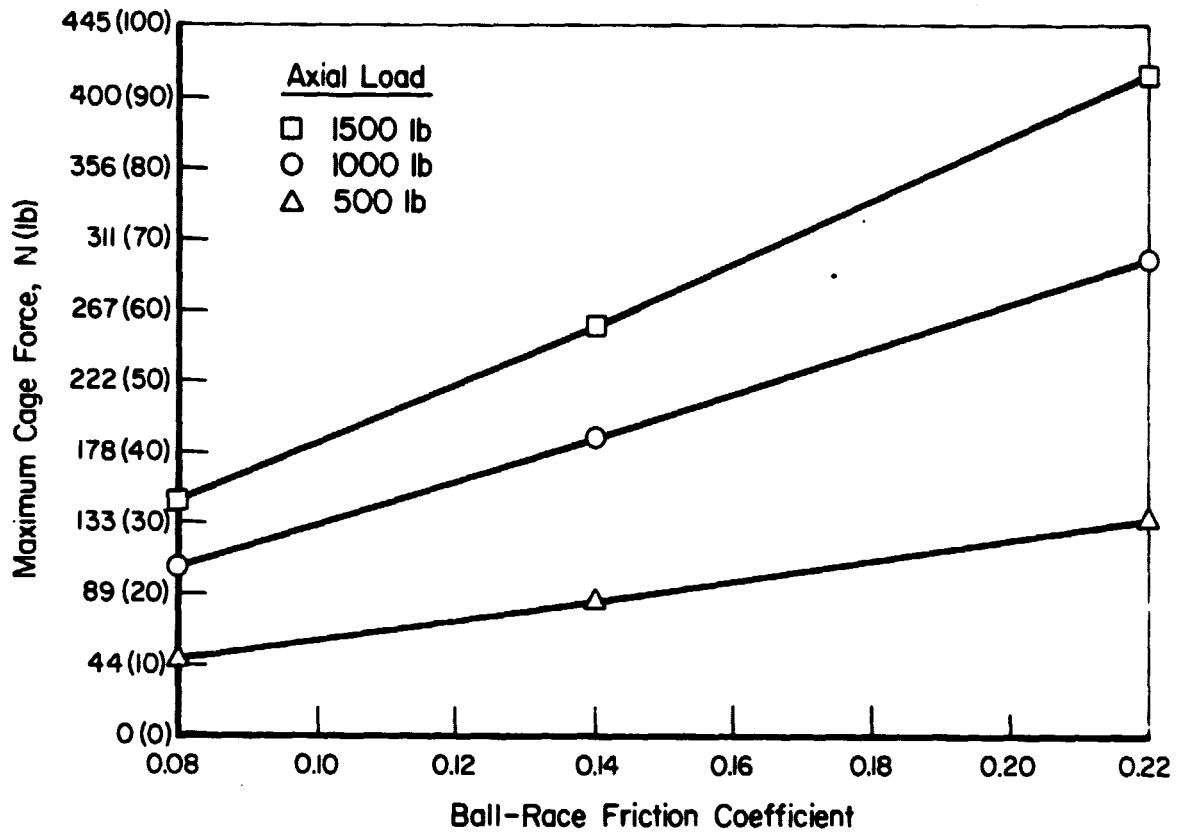
FIGURE 11.   MAXIMUM BALL-CAGE FORCES CAUSED BY BALL-RACE
FRICTION UNDER STABLE OPERATING CONDITIONS

Radial Load = 2669 N (600 lb)          Speed = 31,000 rpm
Cage-Race Friction = 0.13              Ball-Cage Friction = 0.30
Cage-Race Clearance = 0.254 mm         Ball-Cage Clearance = 0.635 mm
   (0.010 in.)                            (0.025 in.)

## Cage Loads Under Abnormal Operating Conditions

### Cage Loads as a Result of Instability

Conditions have been identified in the computer analyses under which the cage might go unstable. Instability can cause high cage stresses from the high accelerations and impacts which develop. An estimate of the acceleration needed to fail the cage can be made from the cage strength for comparison with the accelerations predicted by the computer model, _ ng

$$F = ma \quad,$$

or,

$$a = \frac{F}{M} \quad,$$

where

$a$ = acceleration of cage, mm/sec$^2$ (in./sec$^2$)

$F$ = ball-cage force, N (pounds)

$m$ = cage mass, gm (lb-sec$^2$/in.).

Taking the ultimate compressive force to fail the cage as 5900 N (1300 pounds) and the cage mass of 30 gm (1.7 x 10$^{-4}$ lb-sec$^2$/in.), an acceleration of 2 x 10$^8$ mm/sec$^2$ (8 x10$^6$ in./sec$^2$) is necessary for failure. From the slope of the velocity, $\alpha$, in the unstable plots of Appendix A, such as Figure A-1c, the velocity is seen to change at least 4 x 10$^4$ deg/sec in a quarter of a millisecond, producing accelerations of 10,000 g's. The instantaneous accelerations when the cage strikes the balls are even higher. Therefore, the forces are of the magnitude needed to cause cage failure.

A completely alternate estimation of the forces which arise from cage instability was done after the work of Kingsbury[2]. Kingsbury predicts the forces which arise from the cage whirling about the bearing center. Once again, as in the BASDAP model, the driving force for the instability is energy transferred to the cage from ball-cage interactions. This method predicted a force of 5100 N (1200 pounds), which is also comparable to the cage strength.

Both of these methods predict forces which approach the strength limits of the cage in pure compression. Adding the effects of cage bending, because the forces will probably not produce pure compression, or the summation of forces from several balls would result in instantaneous forces exceeding the strength of the cage. Therefore, cage instability is a likely cause of the cage failure observed.

## Ball Speed Variation

There are several causes for non-uniform ball speeds within a complement and for ball speed variations, including: uneven ball wear, misalignment, cage instability, and a high ratio of radial to axial load. Uneven ball wear causes balls to run at different speeds because of the diameter variations. The HPOTP bearing relies upon either a transfer film from the cage to race or a hydrodynamic film of liquid oxygen in order to lubricate the ball-race interface.[3] An analysis of these mechanisms is currently being conducted at Battelle under Task 112. Preliminary results, both experimental and analytical, indicate very high ball wear rates if the lubrication mechanisms fail. If ball wear is not uniform within the complement, the different resulting ball speeds must be accommodated by ball-race slip.

Misalignment of either race will cause an elliptical path similar to the effect of a high radial load. The effects of race misalignment have been considered under a previous task[4] and, therefore, will not be considered further in this report.

In the HPOTP bearing the combination of axial and radial loads typically cause ball speed variations from contact angle variations around the bearing as much as 14 degrees. As the balls pass over the positions of higher contact angle, they are forced to run faster and so will move forward in the ball pocket. As the balls move to lower contact angles they slow down and lag in the pockets. This effect can cause a detrimental summation of forces if all of the available clearances are consumed in the process. Figure 12 is a plot of the ball excursions from the center of the pocket for a typical case presented in accordance with methods

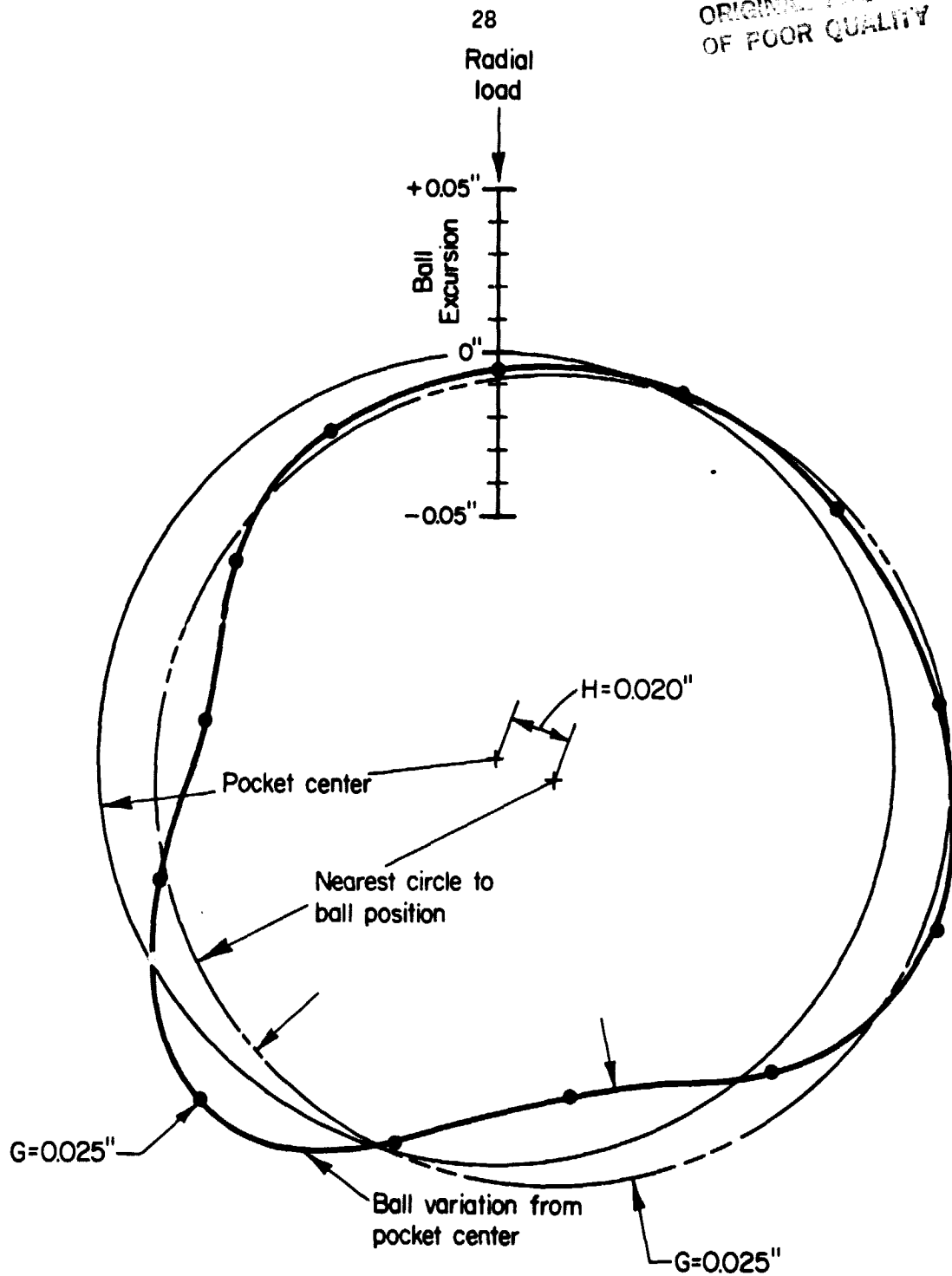FIGURE 12.  BALL EXCURSIONS FROM POCKET CENTER FROM BALL SPEED VARIATION

Axial Load = 4448 N (1000 lb)          Radial Load = 2669 N (600 lb)
Cage-Race Friction = 0.13              Ball-Cage Friction = 0.30
Cage-Race Clearance = 0.254 mm         Ball-Cage Clearance = 0.635 mm
    (0.010 in.)                            (0.025 in.)

of Barish[5]. The irregular curve shows each ball position as calculated
by the BASDAP computer program.

Figure 12 further illustrates the role that cage-race clearance
and ball-pocket clearance play in generating ball-cage forces. The nearest-circle
approximation of the ball set is offset from the pocket center circle
by the distance H. This distance, 0.508 mm (0.020 in.), represents the
distance that the cage center would move to provide a "best fit" for
the ball locations. However, since the cage-race clearance should be
0.25 mm (0.01 in.) for best cage stability, the displacement from the
center can be only 0.13 mm (0.005 in.). The remainder of the distances
of the individual ball excursions must be accommodated by ball-pocket
clearances, represented by the distance G in Figure 12, to prevent ball-race
skidding. For the case in Figure 12, the ball-pocket clearance must
be 0.71 mm (0.028 in.) on either side of nominal or 1.42 mm (0.056 in.)
total. Since the case in Figure 12 is not an extreme example and since
ball-pocket clearance was not shown to affect stability, a ball-pocket
clearance of 2.5 mm (0.100 in.) is probably advisable.

It is seen that several balls in the upper left quadrant of
the graph lag enough, 0.318 mm (0.0125 in.), to be dragged by the cage.
In the lower quadrants, however, two balls lead enough to push the cage.
This situation results in a cage hoop stress such as was described in
an earlier analysis at Battelle[6]. The stress caused by this bending,
however, is limited by the cage to outer race clearance. Calculations
from mechanics of materials[7] indicate that the force from the bending
stress caused by two balls at 180 degrees alternately pushing and dragging
will rise only slightly before the cage-race clearance 0.25 mm (0.010 in.)
will limit any further bending and resulting stress.

A worst case in compression loading might come from a simple
arrangement as shown in Figure 13, where the balls in two quandrants
are leading and in the other two quadrants are lagging. Neglecting friction
at the outer race and summing the forces from six balls in compression
would produce a stress at point A of 70 N/mm$^2$ (10,000 psi). Under the
assumed compressive strength of 230 N/mm$^2$ (33,000 psi), the cage would
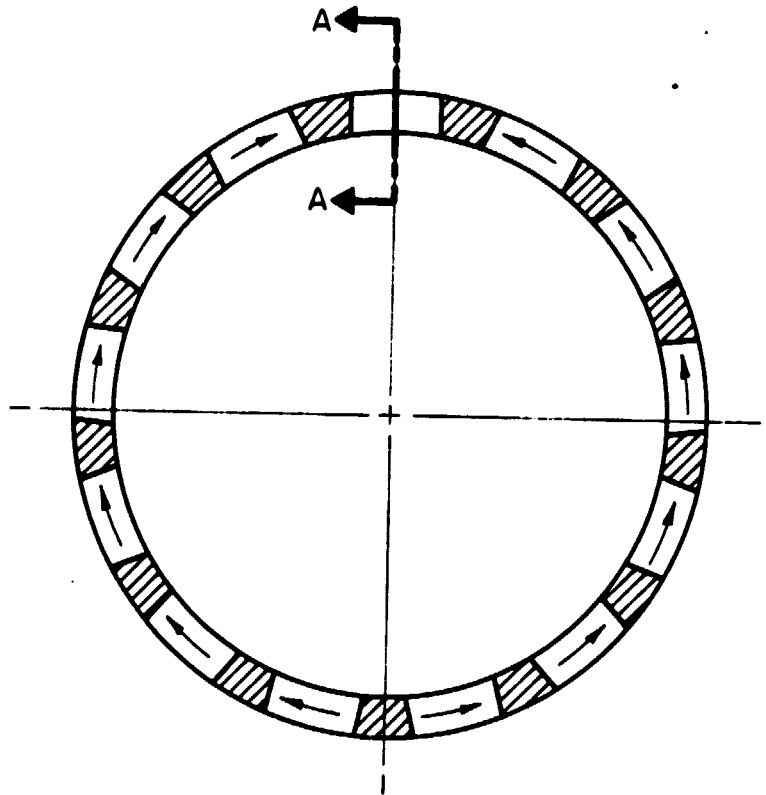still not fail.
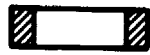
Section A-A



FIGURE 13.   POSSIBLE CAGE LOADING RESULTING
FROM BALL SPEED VARIATION

Other more complex situations can be proposed by envisioning various ball positions leading and lagging in a plot such as in Figure 12. The calculation of the resulting stresses from complex forces and moments in a composite material, restrained by the cage race clearances, was beyond the scope of this task and therefore not considered.

## CALCULATING UNITS

Since the bearing drawing and all input data provided by NASA were in English units, all calculations were performed in English units. Therefore, the SI units presented in this report were converted from English units.

Also, all bearing geometries and clearances given are diametral, unless specified otherwise.

# REFERENCES

1.  Jones, A. B., "A General Theory for Elastically Constrained Ball
    and Radial Roller Bearings Under Arbitrary Load and Speed Conditions",
    Journal of Basic Engineering, pp 309-320, June, 1960.

2.  Kingsbury, E. P., "Torque Variations in Instrument Ball Bearings",
    ASLE Trans., 9, pp 435-441, 1965.

3.  Kannel, J. W., Merriman, T. L., Stockwell, R. D., and Dufrane, K.
    F., "Evaluation of Feasibility of Measuring EHD Film Thickness Associated
    with Cryogenic Fluids", final report to NASA/GCMSFC, August, 1983.

4.  Kannel, J. W., Merriman, T. L., Stockwell, R. D., and Dufrane, K. F.,
    "Evaluation of Outer Race Tilt and Lubrication on Ball Wear and SSME
    Bearing Life Reductions", Final Report to NASA/GCMSFC, July, 1983.

5.  Barish, T., "Ball Speed Variation in Ball Bearings and its Effect
    on Cage Design", J. of Am. Soc. of Lub. Eng., pp 110-116, March,
    1969.

6.  Kannel, J. W., and Merriman, T. L., "SSME Turbopump Bearing Analytical
    Study", final report to NASA/GCMSFC, August, 1980.

7.  Seely, F. B., and Smith, J. O., Advanced Mechanics of Materials,
    2nd Edition, John Wiley & Sons, Inc., New York, p. 182, 1932.

# APPENDIX A

## PLOTS OF CAGE POSITION - ALPHA
## AND CAGE VELOCITY - ALPHADOT
## AS A FUNCTION OF TIME
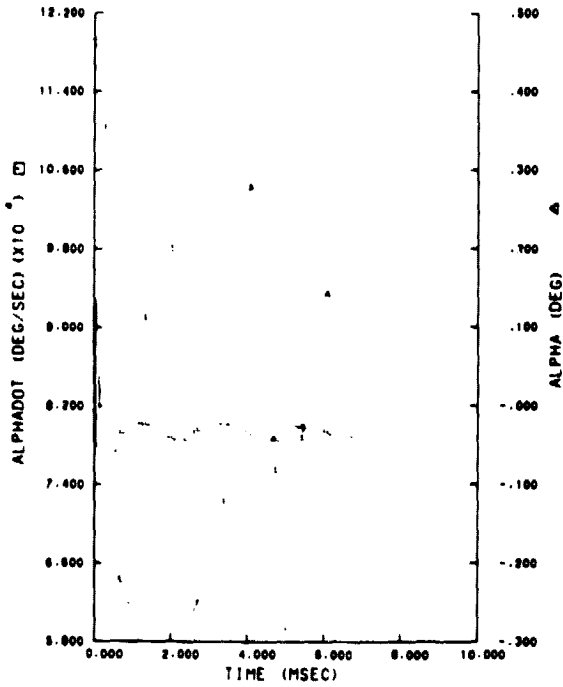
a. Cage-race clearance
0.254 mm (0.010 in.)
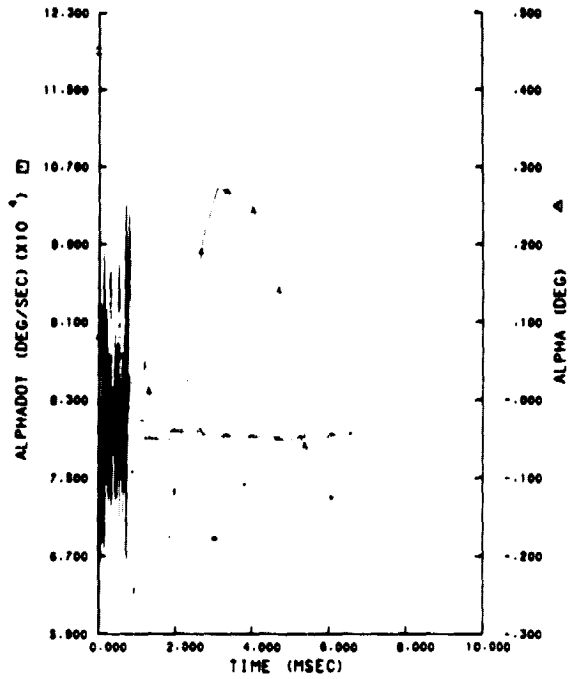
b. Cage-race clearance
0.508 mm ( 0.020 in.)
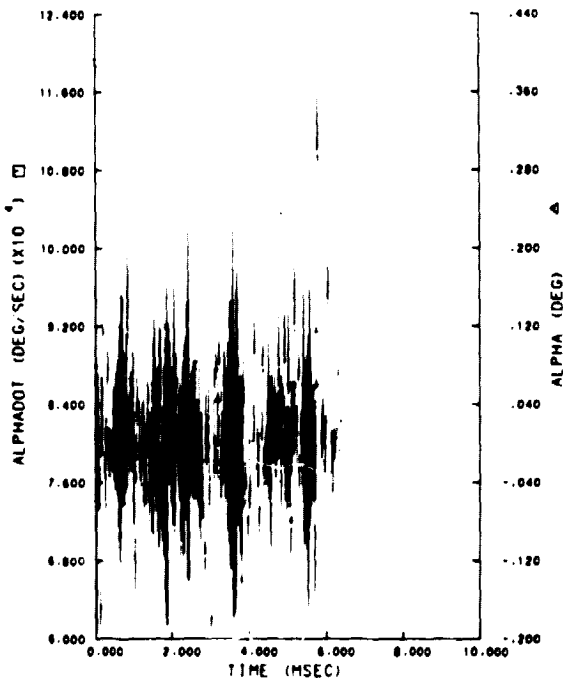
c. Cage·race clearance
0.762 mm (0.030 in.)
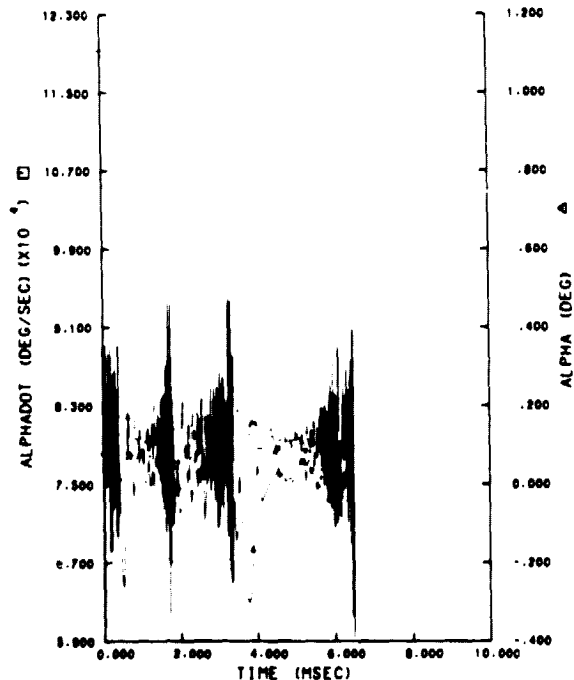
d. Cage-race clearance
1.016 mm (0.040 in.)

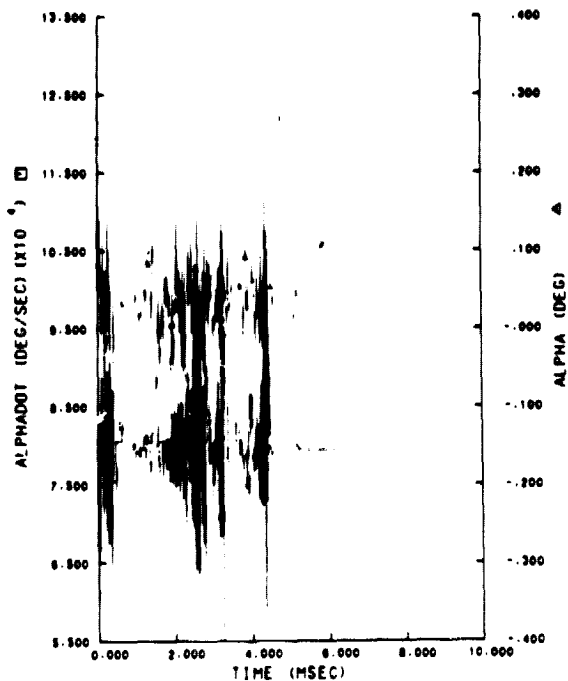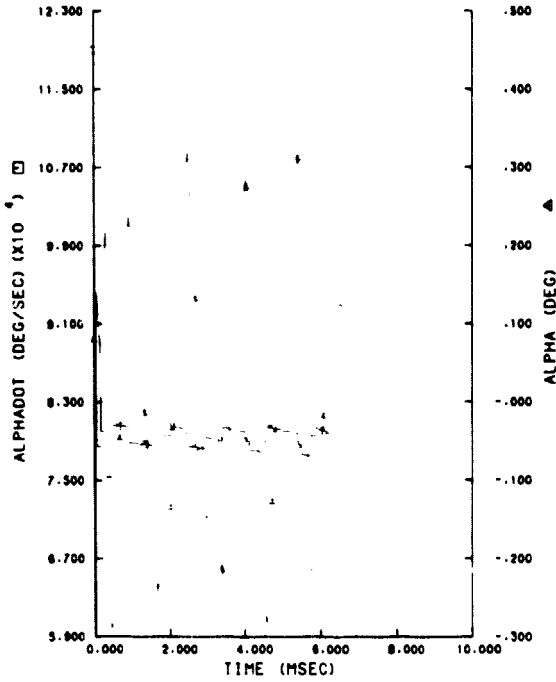FIGURE A-1.   CAGE DYNAMICS AS A FUNCTION OF CAGE-RACE CLEARANCE

Axial Load = 4448 N (1000 lb)
Cage-Race Friction = 0.13
Cage-Race Clearance = Variable
Speed = 31,000 rpm

Radial Load = 2669 N (600 lb)
Ball-Cage Friction = 0.30
Ball-Cage Clearance = 0.635 mm
   (0.025 in.)
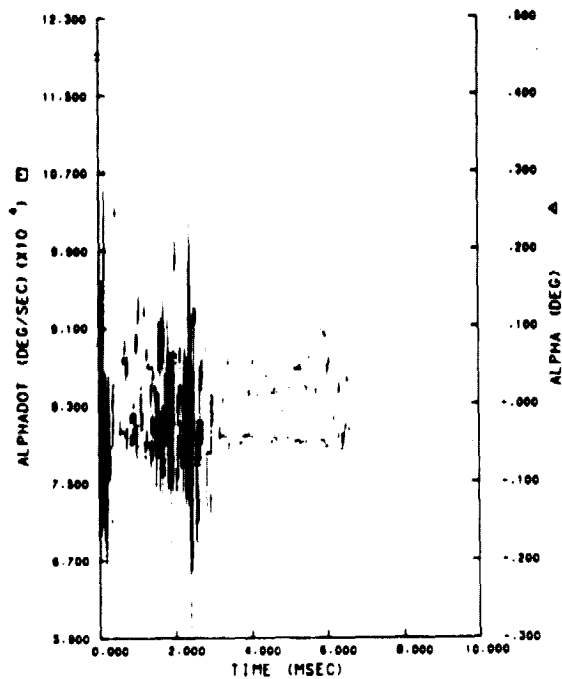
e. Cage-race clearance
1.270 mm (0.050 in.)

f. Cage-race clearance
1.524 mm ( 0.060 in.)

FIGURE A-1. (Continued)
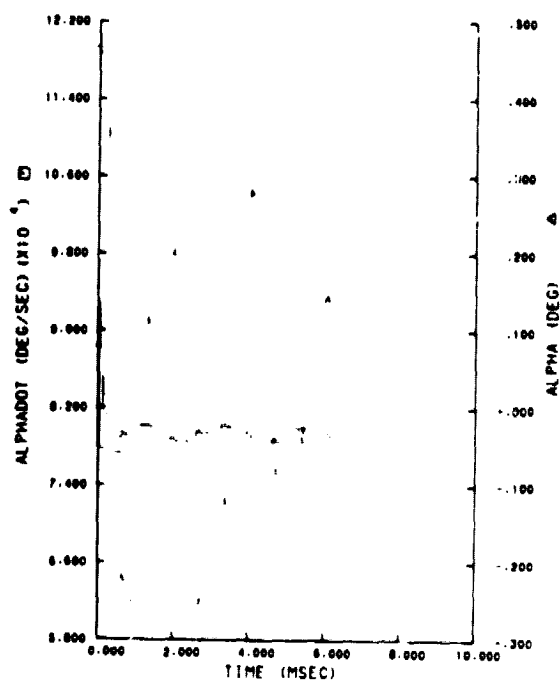
a. Ball-cage clearance
   0.635 mm (0.025 in.)
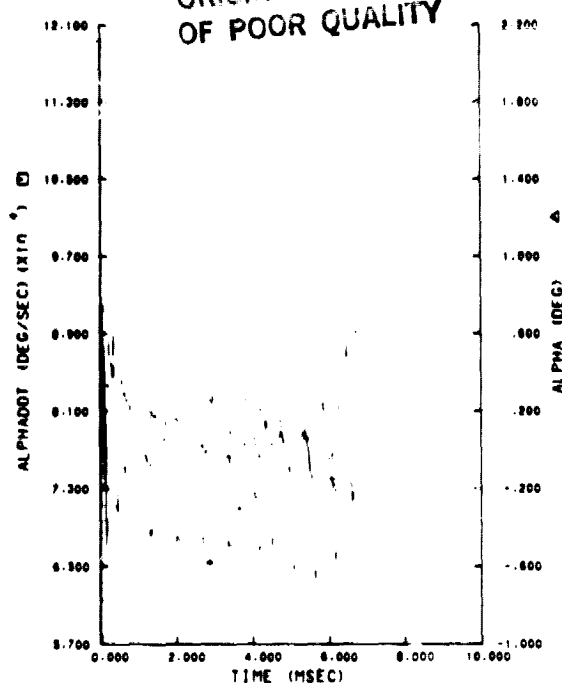
b. Ball-cage clearance
   1.270 mm (0.050 in.)
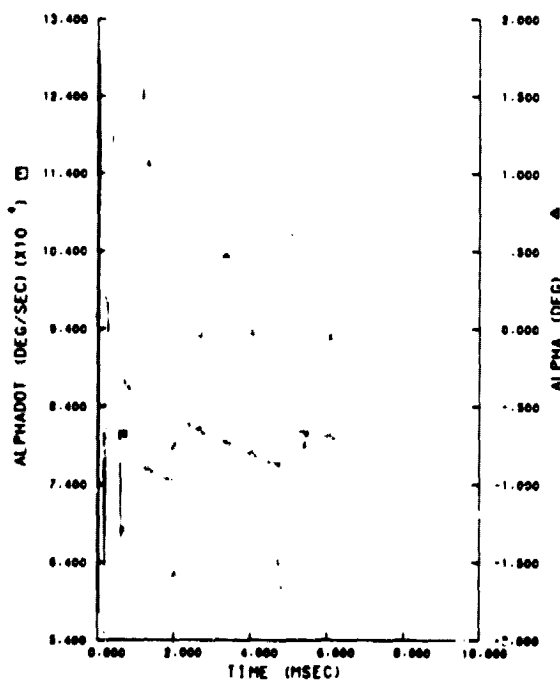
c. Ball-cage clearance
   (2.540 mm (0.100 in.)

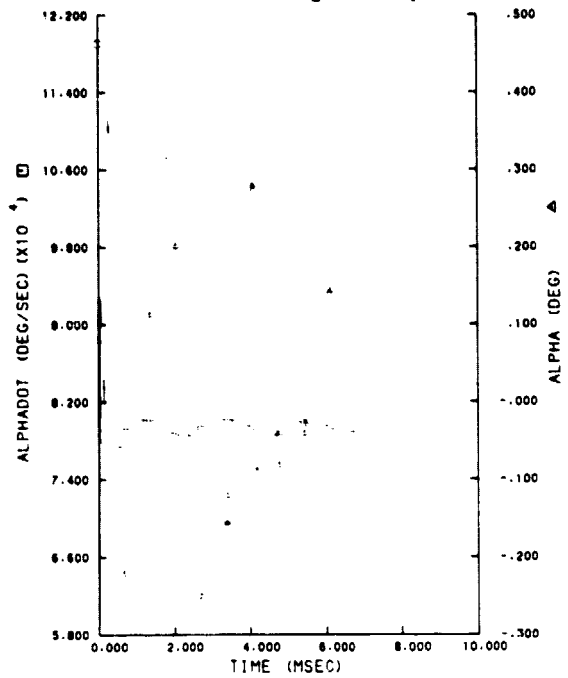FIGURE A-2.  CAGE DYNAMICS AS A FUNCTION OF BALL-CAGE CLEARANCE

Axial Load = 4448 N (1000 lb)
Cage-Race Friction = 0.13
Cage-Race Clearance = 0.254 mm
   (0.010 in.)

Radial Load = 2669 N (600 lb)
Ball-Cage Friction = 0.30
Ball-Cage Clearance = Variable
Speed = 31,000 rpm

a. Cage-race friction
coefficient = 0.04

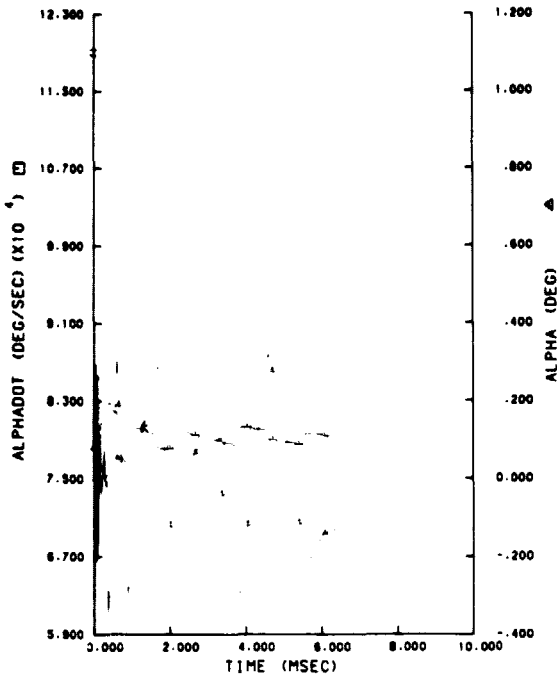b. Cage-race friction
coefficient = 0.13
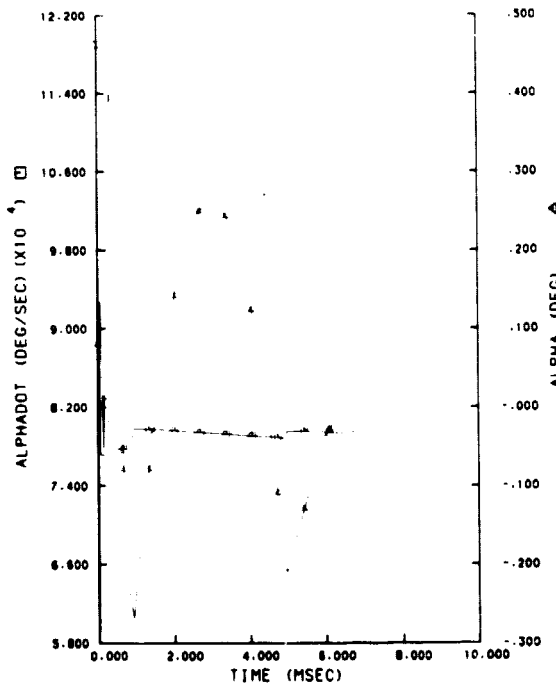
c. Cage-race friction
coefficient = 0.30

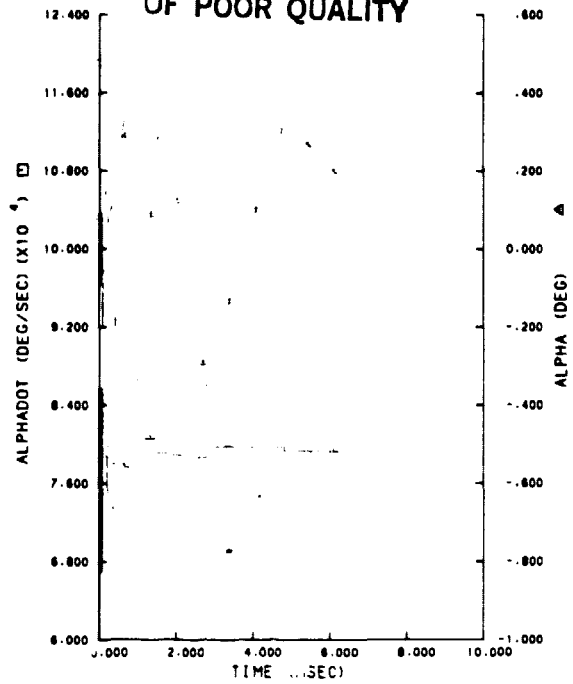FIGURE A-3. CAGE DYNAMICS AS A FUNCTION OF CAGE-RACE FRICTION

Axial Load = 4448 N (1000 lb)
Cage-Race Friction = Variable
Cage-Race Clearance = 0.254 mm
    (0.010 in.)
Speed = 31,000 rpm

Radial Load = 2669 N (600 lb)
Ball-Cage Friction = 0.30
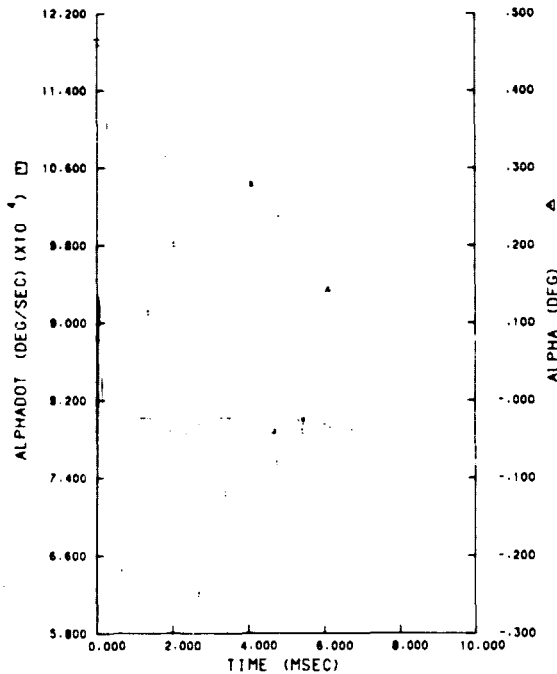Ball-Cage Clearance = 0.635 mm
    (0.025 in.)

a. Ball-cage friction
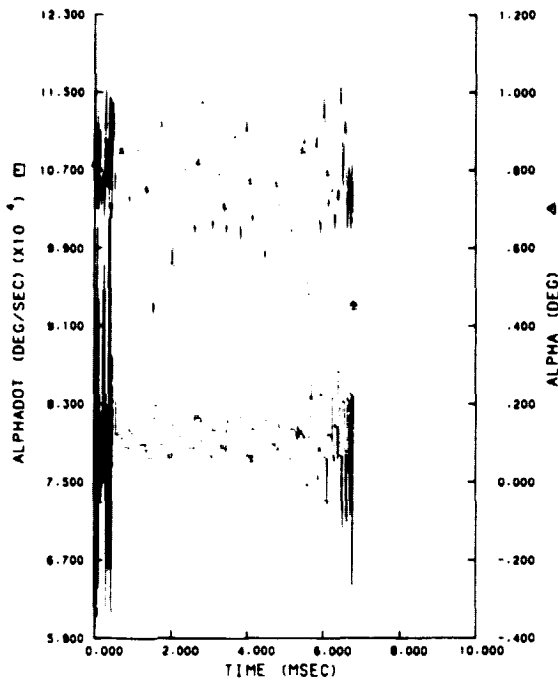coefficient = 0.04

b. Ball-cage friction
coefficient = 0.17

c. Ball-cage friction
coefficient = 0.30

FIGURE A-4. CAGE DYNAMICS AS A FUNCTION OF BALL-CAGE FRICTION

Axial Load = 4448 N (1000 lb)          Radial Load = 2669 N (600 lb)
Cage-Race Friction = 0.13              Ball-Cage Friction = Variable
Cage-Race Clearance = 0.254 mm         Ball-Cage Clearance = 0.635 mm
    (0.010 in.)                            (0.025 in.)
Speed = 31,000 rpm

a. Cage unbalance = 0.019 gm

b. Cage unbalance = 0.094 gm

No Plot Generated
Completely Unstable

c. Cage unbalance = 0.169 gm

d. Cage unbalance = 0.500 gm

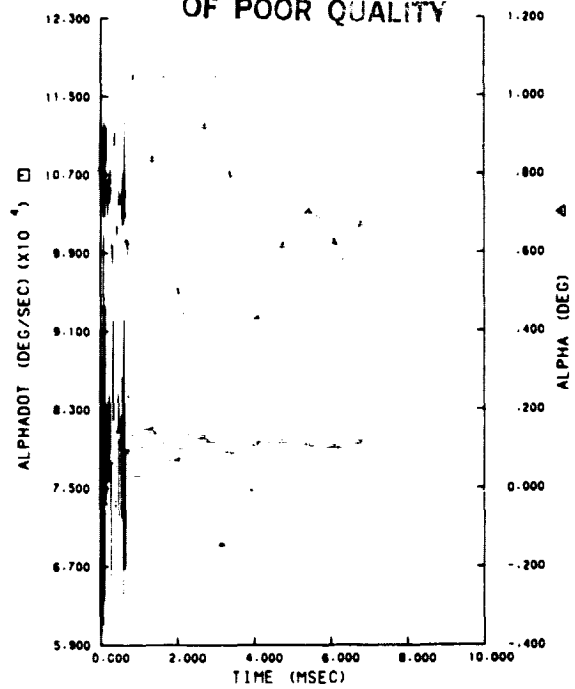FIGURE A-5. CAGE DYNAMICS AS A FUNCTION OF CAGE UNBALANCE

Axial Load = 4448 N (1000 lb)
Cage-Race Friction = 0.13
Cage-Race Clearance = 0.254 mm
   (0.010 in.)
Speed = 31,000 rpm

Radial Load = 2669 N (600 lb)
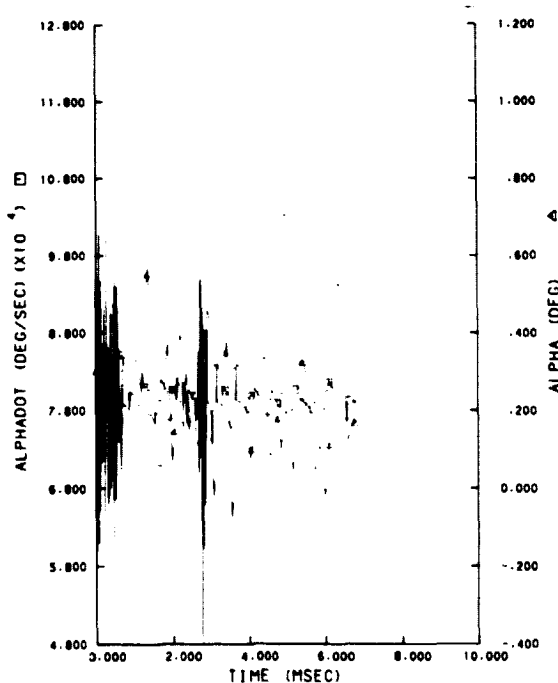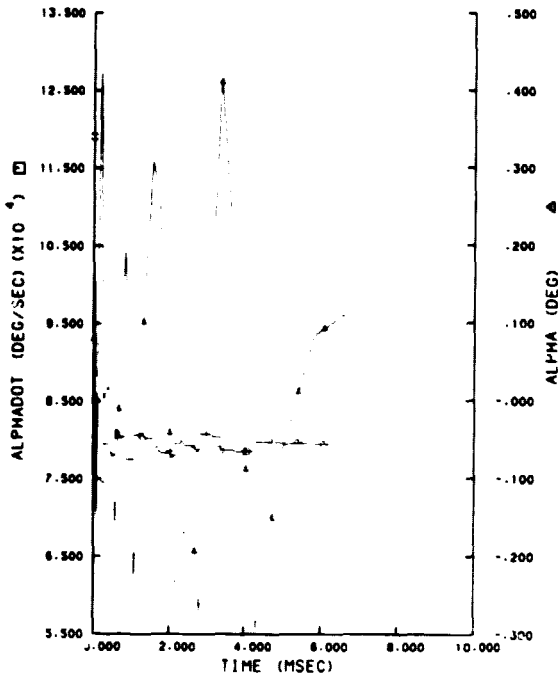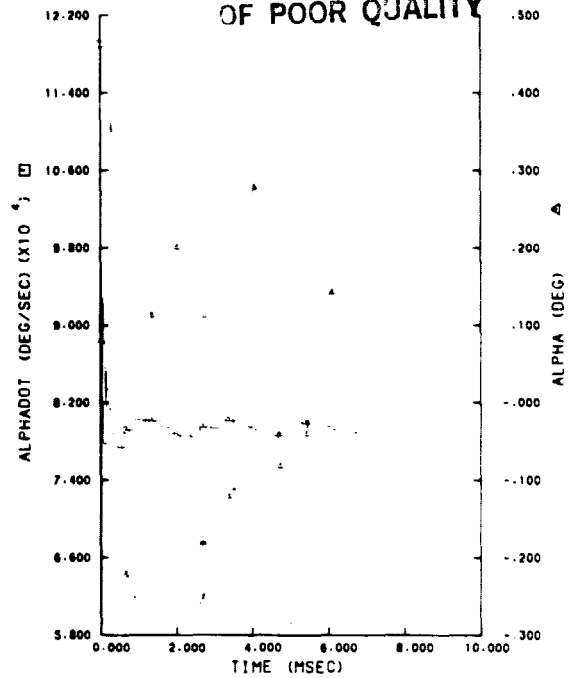Ball-Cage Friction = 0.30
Ball-Cage Clearance = 0.635 mm
   (0.025 in.)

a. Radial load = 890 N (200 lb)



b. Radial load = 2669 N (600 lb)
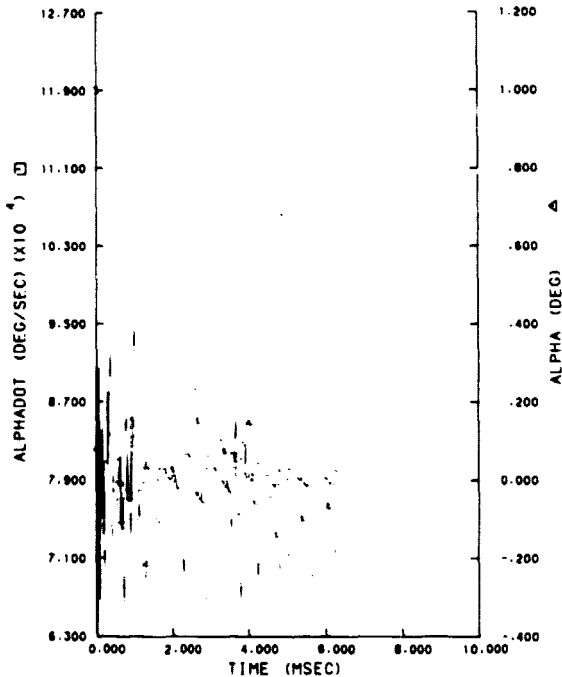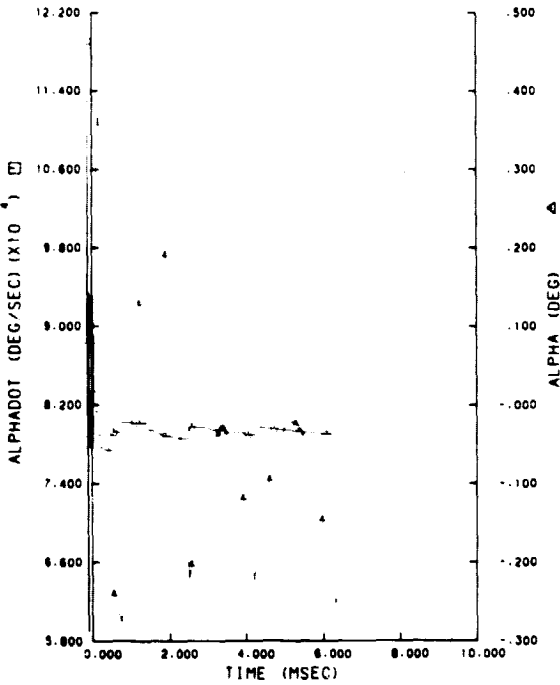


c. Radial load = 4448 N (1000 lb)

FIGURE A-6.   CAGE DYNAMICS AS A FUNCTION OF RADIAL LOAD

Axial Load = 4448 N (1000 lb)          Radial Load = Variable
Cage-Race Friction = 0.13              Ball-Cage Friction = 0.30
Cage-Race Clearance = 0.254 mm         Ball-Cage Clearance = 0.635 mm
    (0.010 in.)                            (0.025 in.)
Speed = 31,000 rpm

a.  Cage mass = 29.00 gm
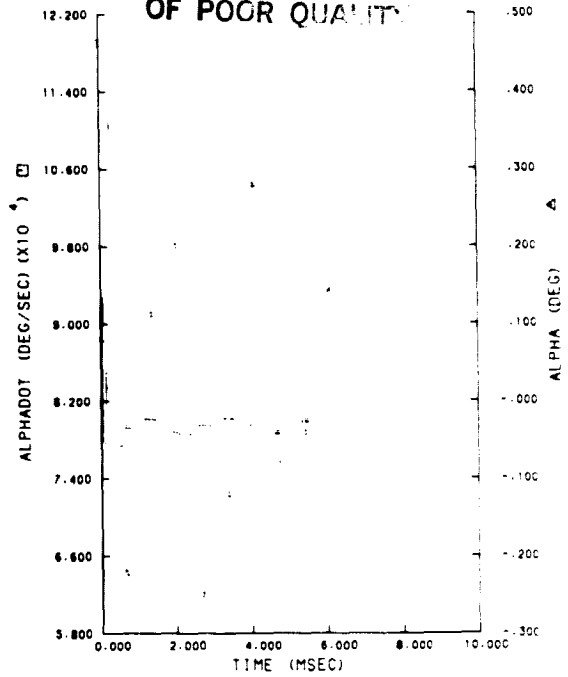
b.  Cage mass = 29.78 gm
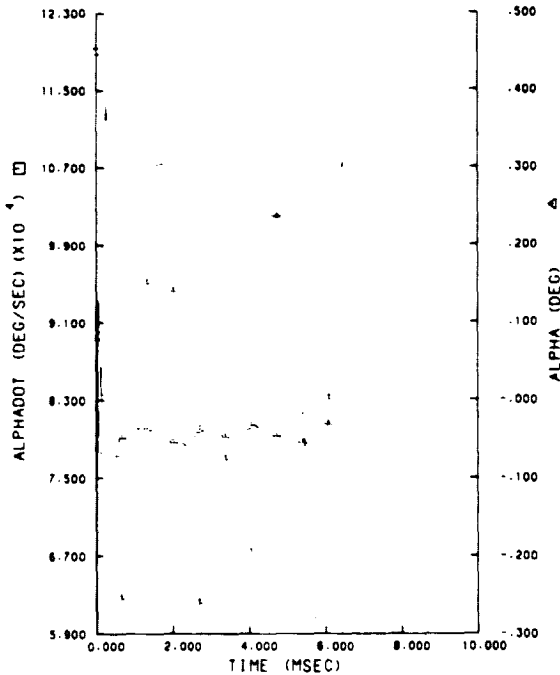
c.  Cage mass = 30.60 gm

FIGURE A-7.  CAGE DYNAMICS AS A FUNCTION OF CAGE MASS

Axial Load = 4448 N (1000 lb)           Radial Load = 2669 N (600 lb)
Cage-Race Friction = 0.13               Ball-Cage Friction = 0.30
Cage-Race Clearance = 0.254 mm          Ball-Cage Clearance = 0.635 mm
    (0.010 in.)                             (0.025 in.)
Speed = 31,000 rpm
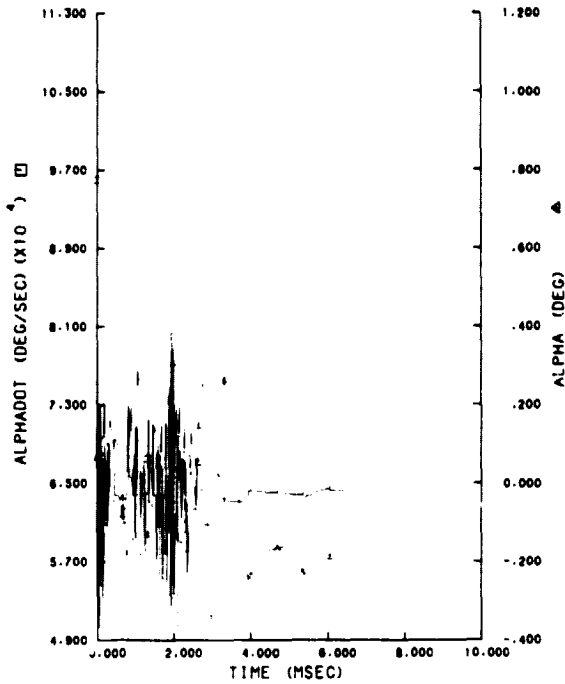
a.  Shaft speed = 25,000 rpm
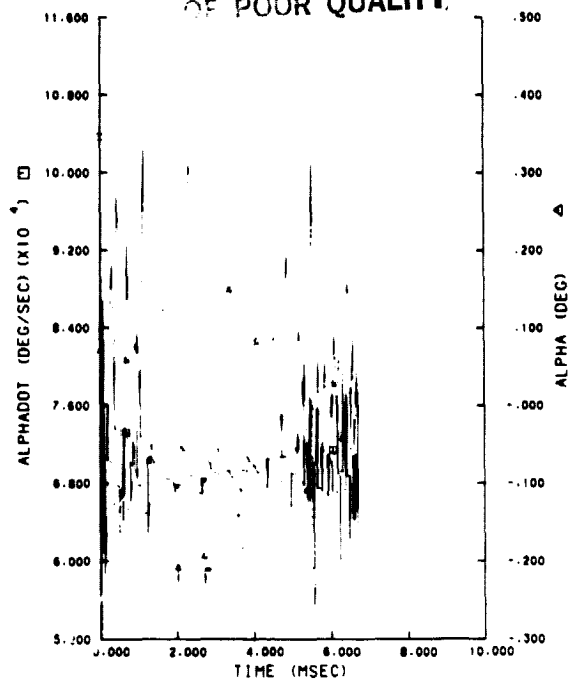
b.  Shaft speed = 27,000 rpm
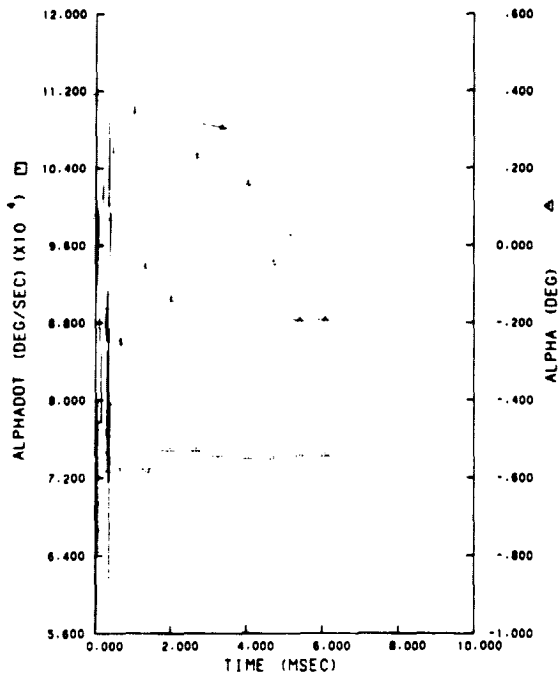
c.  Shaft speed = 29,000 rpm
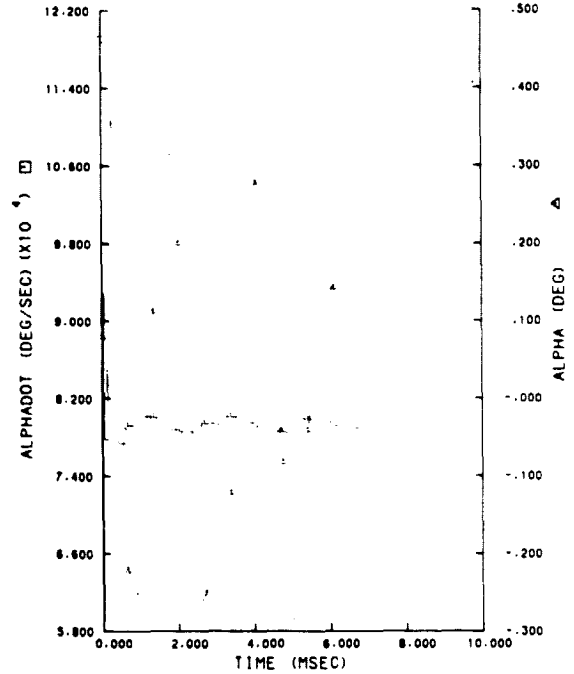
d.  Shaft speed = 31,000 rpm

FIGURE A-8.  CAGE DYNAMICS AS A FUNCTION OF SHAFT SPEED

Axial Load = 4448 N (1000 lb)      Radial Load = 2669 N (600 lb)
Cage-Race Friction = 0.13          Ball-Cage Friction = 0.30
Cage-Race Clearance = 0.254 mm     Ball-Cage Clearance = 0.635 mm
    (0.010 in.)                        (0.025 in.)
Speed = Variable
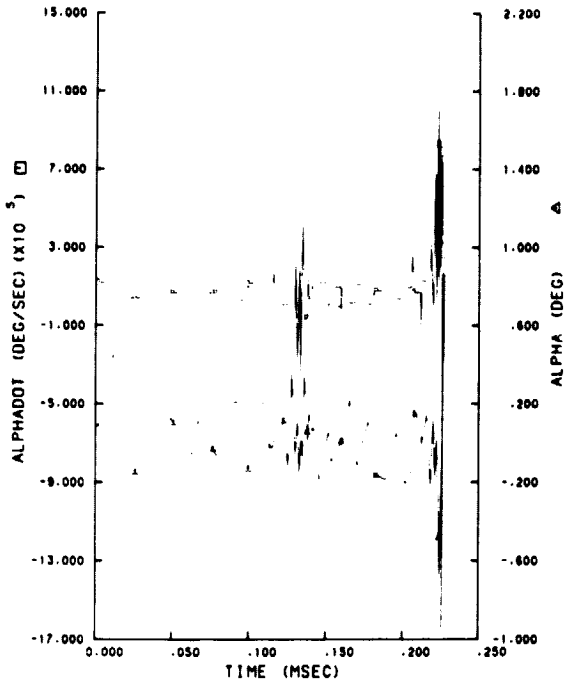
a. Film thickness = 254 x 10⁻⁶ mm
(10 x 10⁻⁶ in.)
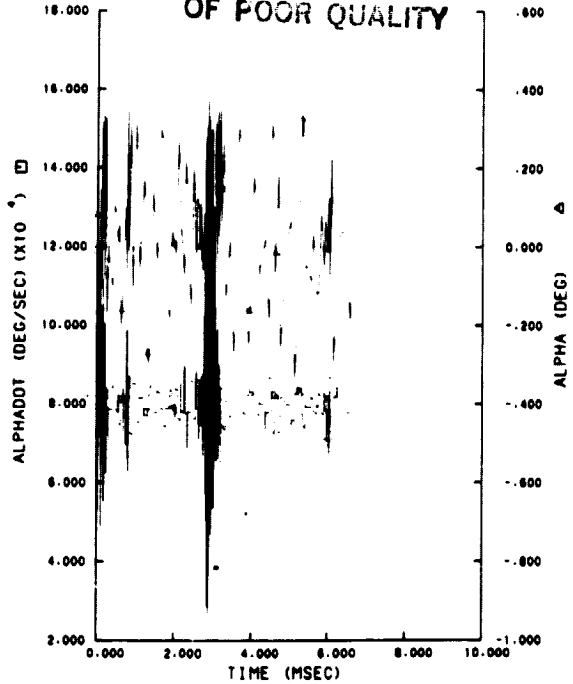
b. Film thickness = 1270 x 10⁻⁶ mm
(50 x 10⁻⁶ in.)
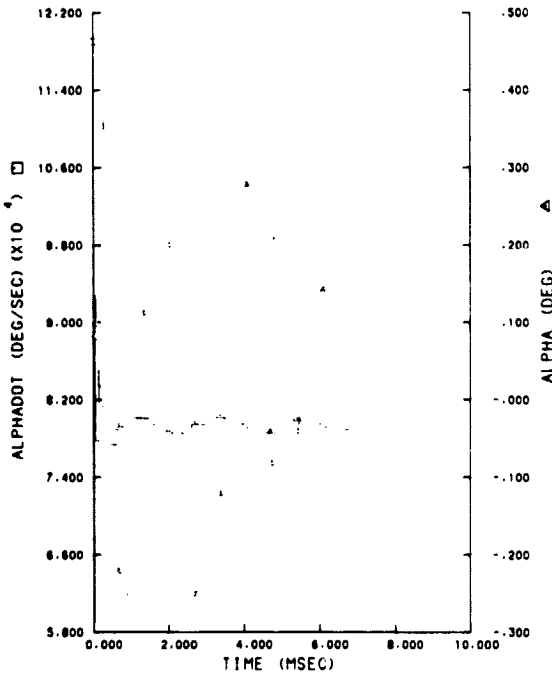
c. Film thickness = 2490 x 10⁻⁶ mm
(98 x 10⁻⁶ in.)

FIGURE A-9. CAGE DYNAMICS AS FUNCTION OF LUBRICANT TRANSFER
FILM EFFECTIVE THICKNESS

Axial Load = 4448 N (1000 lb)          Radial Load = 2669 N (600 lb)
Cage-Race Friction = 0.13              Ball-Cage Friction = 0.30
Cage-Race Clearance = 0.254 mm         Ball-Cage Clearance = 0.635 mm
    (0.010 in.)                            (0.025 in.)
Speed = 31,000 rpm

# APPENDIX B

## THE HIDDEN CAUSE OF BEARING FAILURE

# THE HIDDEN CAUSE OF BEARING FAILURE

Bearing elements sometimes "rattle" in their cage, producing destructive forces that quickly lead to failure. This phenomenon—called cage instability—takes place in a blur of motion that masks the true source of trouble. Here's a new method that pinpoints potentially unstable cages at the design stage.

**J. W. KANNEL**
**D. K. SNEDIKER**
Battelle Columbus Laboratories
Columbus, Ohio

*Cage instability can be identified by the presence of a characteristic, circumferential wear pattern on the inside of the rolling-element pocket. A failed bearing also contains considerable cage wear debris in the ball or roller track and on the bearing shoulders.*



BEARING elements do not fit snugly within their cage but are mounted with a certain amount of clearance. This "play" allows the cage to bounce off the elements repeatedly. If conditions are right, the collisions cause large unstable oscillations in the cage, leading to premature bearing failure.

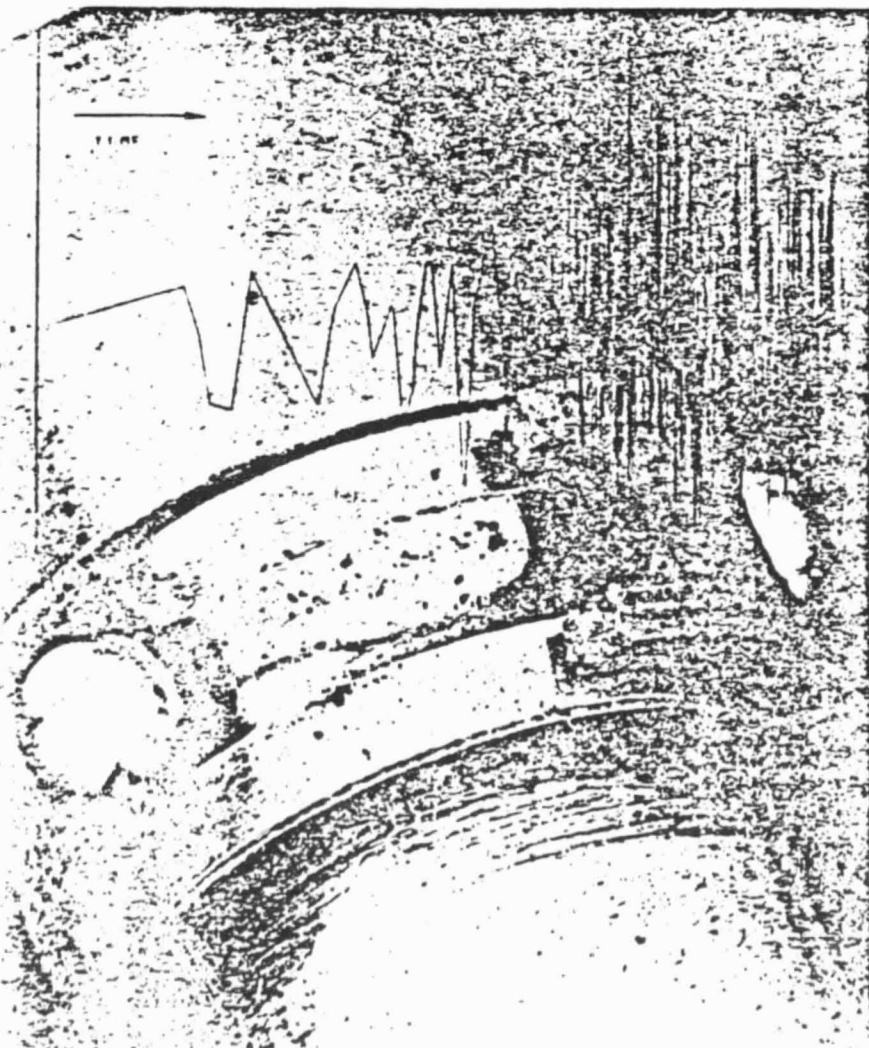Unfortunately, the motion of a cage in a rolling element is difficult to observe, so an unstable cage usually goes undetected. Instead, failures from cage instability are rationalized and blamed on "likely" causes. What's worse, design changes made to correct these "problems" usually aggravate instability.

Cage instability is a recognized problem only in gyroscope and critical aerospace bearings. However, the conditions that cause it are present in many work-a-day bearings such as those used in high-speed machine-tool spindles and textile machines.

There are several ways to recognize cage instability. Perhaps the most obvious sign is an audible noise emitted by the bearing (bearings with unstable cages are often called squealers or groaners). However, most unstable cages do not exhibit this obvious symptom, and more subtle signs of instability must be sought. For instance, an unstable cage causes intermittent torque transients and exhibits a characteristic circumferential wear pattern inside the rolling-element pocket.

Previously, cage instability was difficult to analyze because the dynamic motion of the cage could not be modeled accurately. This article presents a new analytical approach that models cage motion and relates the bearing design and operating conditions to potential cage instability. Thus, a bearing design can be checked before it is

put into service, or bearings that fail consistently can be studied to determine whether cage instability is the underlying cause of failure.

## What Is Cage Instability?

According to conventional theory, a bearing cage is an unconstrained, rigid rotor that rotates circumferentially with the rolling elements. Cage and elements are separated by a thin lubricant film and never touch.

In truth, the cage does not behave this way. Rather, it intermittently impacts one and then another of the rolling elements. Under repeated impact, cage motion either damps out or increases. When motion increases, the cage becomes unstable.

Failure in a bearing depends upon the requirements of the system. Cage instability causes "failure" when its effects on torque, cage life, and bearing noise become unacceptable.

For example, instability causes intermittent torque fluctuations in both low and high-speed bearings. These fluctuations are considered failure in systems requiring smooth operation or accurate positioning. Cage instability also generates severe transient forces that can cause high cage wear or fracture, which eventually disable a bearing. Finally, because an unstable cage sometimes emits noise, it can cause failure in systems requiring quiet operation.

Usually, an unstable bearing leaves some tell-tale physical marks. For instance, a bearing with an unstable cage normally contains a considerable amount of cage wear debris in the ball or roller track and on the bearing shoulders. With nonmetallic cages, instability shows up as a polymer transfer film on the rolling elements.

Failure often appears to be caused by lubricant starvation because the wear debris soaks up oil, robbing the rolling element of lubricant. However, true lubricant starvation results from the rolling element smearing over cage-pocket surface pores thereby blocking the lubricant feed path—little wear debris is present.

## Two Critical Interfaces

Before a dynamic analysis can be performed on a bearing cage, the forces at the rolling-element/race interface and the rolling-element/cage interface must be understood. These forces control whether or not cage motion becomes unstable.

The interface between the element and the race generally represents a typical elastohydrodynamic (EHD) contact. Lubrication is dominated by the hydrodynamic action of the lubricant coupled with elastic deformation of the bearing surfaces. As the lubricant enters the interface region, it undergoes considerable physical change, the most significant change being a large increase in viscosity with increasing pressure. This increase is described by

$$\mu = \mu_i \exp{(\gamma p)}$$

The dominant force at the element/race interface is the tractive force between the element and the race. The magnitude of this force determines the lubricant film thickness and controls whether the element rolls or slips.

In determining tractive force $F_T$, the shear stress in the lubricant film must be found first from

$$\tau = \mu \Delta V / h$$

Then, the total traction at the interface can be expressed as an integral of the shear stress over the contact area. The pressure over the interface normally is represented by a semiellipsoidal (Hertzian) distribution, therefore, tractive force can be expressed as

$$F_T = C_\mu \Delta V \qquad (1)$$

where

$$C_\mu = \frac{3P_L \mu_i}{p_o h (\gamma p_o)^2} \times [(\gamma p_o - 1) \exp{(\gamma p_o)} + 1] \qquad (2)$$

Equation 1 gives the force at the element/race interface for any condition of slip. In effect, the equation represents a classical dashpot model for a simple lubricated interface.

The calculation of damping coefficient $C_\mu$ requires a knowledge of the lubricant pressure-viscosity characteristics and the EHD film thickness. Although several equations are used to calculate film thickness, one commonly used is

$$h = 630 \left[ \frac{\mu U R^{0.375}}{p_o^{1.25}} \right]^{0.727} \qquad (3)$$

where

$$\frac{1}{R} = \frac{1}{R_B} \pm \frac{1}{R_p \mp R_B \cos \beta}$$

$$U = (\Omega/R_p)[R_p^2 - (R_B \cos \beta)^2]$$

The upper signs refer to inner race contact, the lower signs to outer race contact.

At the element/cage interface, the most important force is the spring force between the two parts. When the cage impacts the element, the interface deflects much like a spring under dynamic load. This deflection can be represented by the nonlinear spring equation

$$F = C_s \delta^{3/2} \qquad (4)$$

Spring constant $C_s$ can be calculated from

$$C_s = \frac{0.49}{\sqrt{A_s + B_s}} \left( \frac{B_s}{A_s} \right)^{0.45} \times \left( \frac{1}{C_B + C_p} \right) \qquad (5)$$

For a steel bearing, variables $A_s$, $B_s$, $C_B$, and $C_\nu$ are given by

$$A_s = \frac{1}{2}(R_B^{-1} - R_{cp}^{-1})$$
$$B_s = (2R_B)^{-1} \qquad (6)$$
$$C_p = 0.9/E_c$$
$$C_B = 4.1 (10^{-12}) \; m^2/N$$

The magnitude of spring force $F$ determines the rebound mo-

tion of the cage. Depending on the rebound force, cage motion may be either damped out or accelerated.

For the stability calculations, Equation 4 can be approximated more conveniently with a linear form

$$F = C_{sl}\delta$$

One way to estimate $C_{sl}$ is to assume that the linear and nonlinear force equations yield the same deflection at a charac-

teristic load. For example, at a load of 5 N

$$C_{sl} = (5C_s^2)^{1/3}$$

Performing similar calculations over a range of load values yields similar relationships between $C_s$ and $C_{sl}$.

## Element/Cage Impact

During impact between the cage and a rolling element, a force is exerted on the cage that is proportional to the spring

rate of the interface (Equation 4) and to rolling-element slippage (Equation 1). This force gives the cage a linear velocity normal to the element at the point of impact. The interaction between the element and the cage can be expressed by the fundamental motion equation

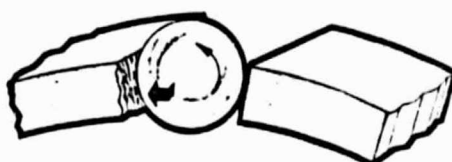$$\ddot{\delta} + \frac{C_{sl}}{2C_s}\dot{\delta} + C_{sl}\delta = 0$$

which applies for the duration of impact.

---

# How the Trouble Starts
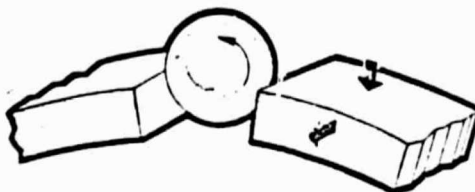
### Elements Hit the Cage
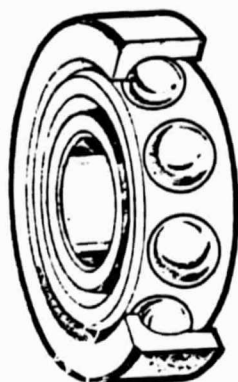
IMPACT

REBOUND



Spin of rolling element imparts tangential force to cage.
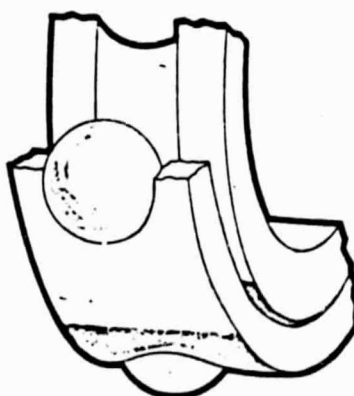
Cage moves down and away from bearing element.

### Impacts Lead to Instability



Repeated impact bounces cage back and forth between elements.

Or cage may move sideways out of bearing plane.
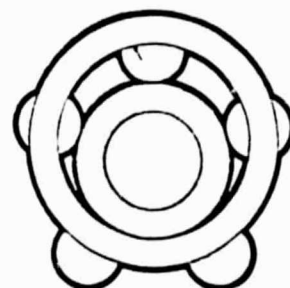
Cage may also spin about center other than bearing center.

### Interface Forces Control Cage Motion



Lubricant

High-pressure region
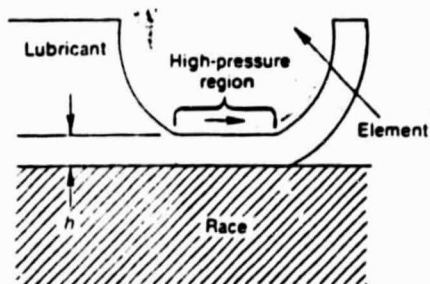
Element

Race

ELEMENT/RACE INTERFACE

In a classic EHD region, traction force depend on contact pressure, lubricant film thickness, and sliding velocity. Traction force determines whether the bearing element rolls or slides.

Element

Cage

$v_s$
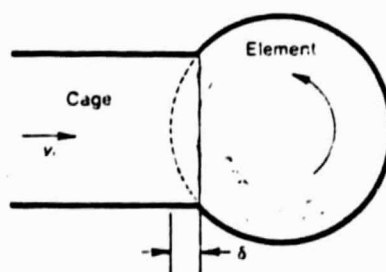
ELEMENT/CAGE INTERFACE

Cage acts like a nonl. spring Spring force determines cage rebo velocity and, thus, wh cage motion damps c increases.

Defining restitution factor $e_c$ as

$$e_c = \exp\left(-\frac{\pi}{\sqrt{D_p - 1}}\right) \qquad (7)$$

where

$$D_p = \frac{32C_r^2}{MC_{sl}} \qquad (8)$$

it can be shown that the rebound cage velocity $v_r$ is

$$v_r = -e_c v_i \text{ for } D_p > 1$$
$$v_r = 0 \text{ for } D_p \leq 1$$

Thus, for low values of $D_p$ (less than 1), the cage will not rebound from an impact but will lose its forward momentum. On the other hand, for values of $D_p$ greater than 1, momentum can increase because of the friction at the element/race contact. In other words, the cage not only rebounds, it also accelerates tangentially to the element surface in the direction of rotation.

Large values of $D_p$, therefore, *imply* cage instability because cage oscillations are accelerated. However, simply knowing that $D_p$ is large is not sufficient evidence on which to judge the stability of a cage. More information about the impact is needed because although the cage rebounds, it is not known whether the cage has more or less energy than before the impact.

The full dynamic behavior of a cage requires extensive calculations that can be carried out only on a computer. Actual dynamic calculations trace the cage position as a function of time in a series of discrete time steps. Calculation of the momentum change of the cage after an impact is based upon the resitution factor and the friction level at the element/cage interface.
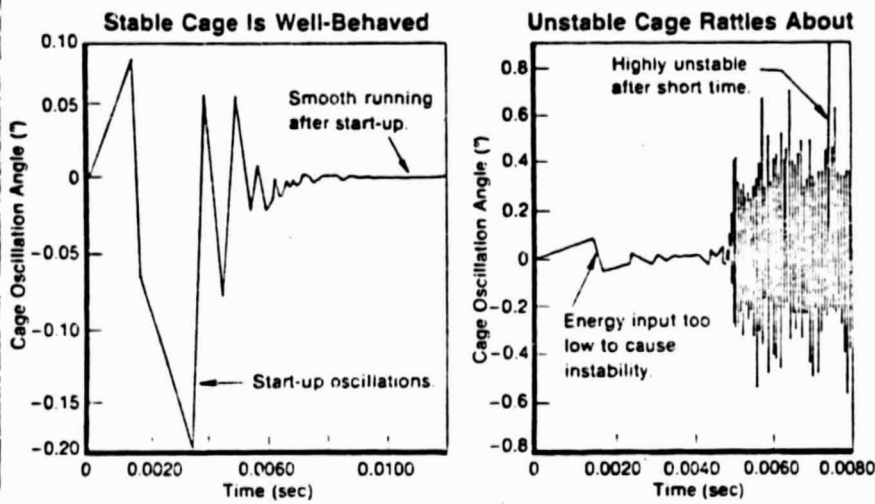
The effects of the restitution factor have been fairly well modeled. However, the effects of friction are more difficult to generalize in a simple equation. But a model using a simple four-ball bearing configuration, where the cage moves sequentially from ball to ball, has yielded a satisfactory relationship between restitution factor and friction. This relationship is illustrated in the stability plot and provides a convenient criterion for predicting cage instability.

To determine whether a cage is unstable, first find the restitution factor $e_c$ and the coefficient of friction between the rolling element and the cage. Then, locate these values on the stability plot. If the plotted point falls below the line, the cage is stable. However, if the point falls above the line, the cage is unstable.

## Checking a Bearing

In general, to determine the stability of a bearing cage, the following parameters must be known:

- Cage pocket radius, $R_{cp}$.



**Stable Cage Is Well-Behaved**

Smooth running after start-up.

Start-up oscillations

**Unstable Cage Rattles About**

Highly unstable after short time.

Energy input too low to cause instability

**Quick Check of Stability**
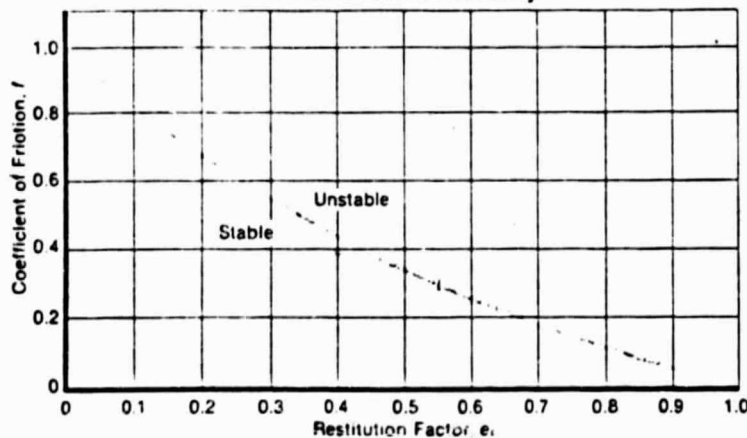
Unstable

Stable

To check the stability of a cage, first determine the coefficient of friction and the restitution factor. Then, plot these values on the graph. If the plotted point falls below the line, the cage is stable.

## Pressure-Viscosity Properties for Typical Lubricants

| | at 65°C | | | at 95°C | | | at 150°C | | |
|---|---|---|---|---|---|---|---|---|---|
| Lubricant | $\mu$ (N·m/sec²) | $\mu_i$ (N·m/sec²) | $\gamma$ (m²/N × 10⁻¹⁰) | $\mu$ (N·m/sec²) | $\mu_i$ (N·m/sec²) | $\gamma$ (m²/N × 10⁻¹⁰) | $\mu$ (N·m/sec²) | $\mu_i$ (N·m·sec²) | $\gamma$ (m²/N × 10⁻¹⁰) |
| SAE 10 | 0.011 | 300 | 4.6 | 0.0052 | 90 | 4.6 | 0.002 | 40 | 4.6 |
| SAE 30 | — | — | — | 0.011 | 180 | 5.9 | 0.0032 | 49 | 5.9 |
| MIL-L-23699 (Ester) | 0.012 | 1.2 | 26.6 | 0.0057 | 0.20 | 26.6 | 0.0024 | 0.020 | 26.6 |
| MIL-L-7808 (Ester) | 0.0055 | 0.22 | 27.1 | 0.0031 | 0.09 | 27.1 | 0.00155 | 0.0085 | 27.1 |

- Pitch radius, $R_p$.
- Rolling-element radius, $R_a$.
- Contact angle, $\beta$.
- Rotational speed, $\Omega$.
- Maximum contact pressure, $p_o$.
- Load per rolling element, $P_L$.
- Cage mass, $M$.
- Elastic modulus of cage material, $E_c$.
- Coefficient of friction between rolling element and cage, $f$.
- Base viscosity of lubricant, $\mu$.
- Intercept viscosity, $\mu_i$.
- Pressure-viscosity exponent, $\gamma$.

Most of these parameters are routinely available; however, the last two parameters require some data manipulation before they can be determined.

These parameters describe the variations of viscosity with pressure based on the ideal EHD model. To determine them, the pressure/viscosity data of a lubricant must be plotted. The point where the plot crosses the viscosity axis is the intercept viscosity $\mu_i$, and the slope of the plot at this point is the pressure-viscosity exponent $\gamma$. (Typical values of $\mu$, $\mu_i$, and $\gamma$ for four lubricants are listed in the table.)

Once all the design parameters are known, the following variables must be calculated:
1. EHD film thickness, $h$
2. Damping coefficient, $C_\mu$.
3. Spring constant, $C_{sl}$.
4. Stability factor, $D_\mu$.
5. Restitution factor, $e_c$.

If $D_\mu$ is greater than 1, some cage instability can be expected. However, if friction factor, $f$ is small, the cage may still operate in a stable mode. But the higher the viscosity or friction and the smaller the film thickness, the greater the tendency for instability.

For example, consider a machine-tool-spindle bearing with 11 rolling elements and a phenolic cage, operating at 4,000 rpm under an axial load of 500 N. The bearing is lubricated with MIL-L-23699 oil at 65°C. but the lubricant conditions are not certain and could range from 100% to 10% predicted film. Determine if the cage is stable.

The input parameters are $R_{cp}$ = 0.0041 m, $R_p$ = 0.024 m, $R_a$ = 0.004 m, $\beta = 30°$, $p_o = 1.19(10^9)$ N/m², $P_L$ = 90.9 N/ball, $M$ = 4.7 g, $E_c = 7.56(10^8)$ N/m², $\mu$ = 0.012 N-m/sec², $\mu_i$ = 1.2 N-m/sec², and $\gamma = 26.6(10^{-10})$ m²/N. Preliminary calculations give $U$ = 10 m/sec and $R$ = 0.0033 m.

At 100% predicted film, lubricant film thickness (from Equation 3) is $h$ = 0.16 $\mu$m. Damping coefficient (Equation 2) is $C_\mu$ = 8.97 N-sec/m, and linearized spring constant (Equations 5 and 6) is $C_{sl}$ = 5.7(10⁵) N/m. Finally, stability factor (from Equation 8) is $D_\mu$ = 0.96. Because $D_\mu$ < 1, the bearing cage is stable at 100% predicted film thickness.

If, however, the lubricant film is only 10% of the predicted film, then $h = 0.016\mu$m and $D_\mu$ = 96. Thus, the cage could be unstable depending on the relationship between the friction factor and restitution factor.

Friction factor for this condition typically exceeds 0.20, and restitution factor is

$$e_c = \exp\left(-\frac{\pi}{\sqrt{96-1}}\right)$$
$$= 0.72$$

Plotting these values on the stability graph indicates that this cage has a stability problem at 10% predicted film. **MD**

### Nomenclature

$A_i, B_i, C_a, C_p$ = Calculation constants
$C_t$ = Spring constant of rolling-element interface
$C_{al}$ = Linearized spring constant
$D_\mu$ = Stability factor
$E_c$ = Elastic modulus of cage material
$e_c$ = Restitution factor
$F$ = Spring force between rolling element and cage
$F_\tau$ = Tractive force
$f$ = Coefficient of friction
$h$ = EHD film thickness
$M$ = Cage mass
$P_L$ = Applied load per rolling element
$p$ = Pressure
$p_o$ = Maximum Hertz contact pressure
$R$ = Relative radii
$R_a$ = Rolling element radius
$R_{rp}$ = Cage pocket radius
$R_p$ = Bearing pitch radius
$U$ = Sum velocity of rolling contact
$\Delta V$ = Slip velocity
$v_i$ = Initial velocity of cage
$v_r$ = Cage rebound velocity
$\beta$ = Bearing contact angle
$\gamma$ = Pressure-viscosity coefficient
$\delta$ = Deflection at rolling-element/cage interface
$\mu$ = Lubricant viscosity
$\mu_i$ = Intercept viscosity
$\tau$ = Shear stress in lubricant film
$\Omega$ = Rotational speed